



OPEN A reappraisal of cell cycle phase enrichment in synchronized estrogen receptor-positive cell models derived from breast adenocarcinomas

Pelin Toker^{1,4}, Hazal Ayten^{1,4}, Öykü Deniz Demiralay^{1,2,4}, Büşra Bınarcı^{1,4}, Gizem Turan¹, Çağla Ece Olgun¹, Pelin Yaşar^{1,3}, Hesna Begüm Akman¹ & Mesut Muyan¹✉

17 β -estradiol (E2), the main circulating estrogen hormone, is a critical signaling factor for the growth, differentiation, and function of breast epithelial cells. The effects of E2 on the breast tissue are primarily mediated by the estrogen receptor α (ER α). Deregulation of the E2-ER α signaling contributes to the initiation/progression of breast cancer and resistance to treatments. Cell lines from breast adenocarcinomas as in vitro model systems provide invaluable insight into cellular events, drug discovery, and drug resistance. Among ER α -synthesizing cell lines, MCF7 and T47D cells are widely used to elucidate cell cycle phase-specific molecular events that coordinate cellular proliferation mediated by E2-ER α . Due to variable results in generating phase-enriched populations with various approaches, we wanted to reassess cell cycle synchronization-coupled phase enrichment with charcoal dextran-treated fetal bovine serum, CD-FBS, as an effective hormone withdrawal approach, alone or in combination with excess thymidine, as a DNA replication inhibitor, and/or nocodazole, a microtubule poison, in MCF7 and T47D cells. We find that hormone withdrawal synchronizes both MCF7 and T47D cells at the G0/G1 phase. Supplementation of CD-FBS with E2 enriches the S phase population. E2 with nocodazole and nocodazole-coupled mitotic shake-off augments the G2/M phase population of MCF7 cells. However, the double thymidine block approach with nocodazole or nocodazole-coupled mitotic shake-off is more effective in enriching S and G2/M phase populations of T47D cells. Our results highlight the differential efficacy of synchronization approaches in MCF7 and T47D cells that could provide a framework for cell cycle-specific applications in breast cancer research.

Keywords Breast cancer, Cell cycle, Estrogen, Synchronization

The progression of the cell cycle for cellular proliferation involves an integrated series of transcriptomic, epigenomic, proteomic, and metabolomic processes that are dynamically and temporally regulated in response to various signaling^{1–4}. 17 β -estradiol (E2) as the main circulating estrogen hormone is a critical signaling factor for the growth, differentiation, and function of reproductive, cardiovascular, musculoskeletal, immune, and central nervous systems^{5,6}. E2 exerts its effects on cells of target systems through transcription factors, estrogen receptor (ER) α and ER β encoded by distinct genes. ER α is the predominant regulatory protein in breast tissue⁶. Although ER α is mainly present in the nucleus, a fraction of ER α is also localized at the plasma membrane and mitochondria^{7–10}. The presence of ER α in various locations in cells implies that the exertion of E2 effects on cellular phenotypes involves dynamically integrated and finely tuned ER α -mediated signaling cascades. The so-called “extra-nuclear” E2 signaling mediates the second-to-minute (or rapid) transcription-independent effects of ER α and also post-translationally modulates the functions of nuclear ER α , transcription

¹Department of Biological Sciences, Middle East Technical University, 06800 Çankaya-Ankara, Türkiye. ²Paul Langerhans Institute Dresden (PLID) of Helmholtz Center Munich at the University Clinic Carl Gustav Carus of TU Dresden, Helmholtz Zentrum München, German Research Center for Environmental Health, Neuherberg, Germany. ³Current Address: Epigenetics and Stem Cell Biology Laboratory, Single Cell Dynamics Group, National Institute of Environmental Health Sciences, Research Triangle Park, NC 27709, USA. ⁴Pelin Toker, Hazal Ayten, Öykü Deniz Demiralay and Büşra Bınarcı contributed equally. ✉email: mmuyan@metu.edu.tr

factors, co-regulatory proteins, and chromatin complexes leading to delayed responses. The contribution of the endoplasmic reticulum membrane localized G protein-coupled estrogen receptor, also known as GPR30, to rapid E2 signaling notwithstanding¹¹, the binding of E2 to the plasma membrane-associated ER α induces the activation of the ERK/MAPK and/or PI3K/AKT signaling cascades that contribute to various cellular processes including proliferation and migration^{12–15}. Nevertheless, the ‘delayed or protein synthesis-dependent’ nuclear E2-ER α signaling is the critical determinant to phenotypical changes in target cells^{5,6}. E2-ER α regulates the expression of target genes that encode proteins involved in nucleic acid and protein metabolism, transcription factors, membrane signaling pathways, and receptor proteins. This regulation orchestrates DNA replication, repair, and progression through the cell cycle^{16–18}. Deregulation of the E2-ER α signaling contributes to the initiation and development of estrogen-target tissue malignancies, including breast cancer^{5,6}.

A better understanding of the sequence of events that coordinate cellular proliferation in response to the E2-ER α signaling could significantly contribute to developing effective prognostic tools and therapeutic interventions for target tissue malignancies. This necessitates the identification of factors and the delineating of their functions in the initiation and progression of cell cycle phases that culminate in cell division. Approaches, with varying advantages and disadvantages, are centered around physical fractionations and chemical/pharmacological agents to synchronize the passage of cells through the cell cycle as a means to enrich cells in each phase^{19–21}. Physical fractionation techniques are based on the size and density of cells by centrifugal separation as well as light scatter or fluorescent emission of labeled cells using a flow cytometer or fluorescence-activated cell sorter. Because of nonuniform size distributions of tumorigenic cells due to polyploidy, low cellular yields, and dependency on specialized equipment in physical fractionation techniques, chemical/pharmacological agents that primarily target DNA synthesis or mitotic spindle formation for the transient inhibition of cell cycle phase transitions have been widely used for synchronization studies^{19–21}.

We have been involved in studies that aim at understanding the mechanisms of E2-ER α signaling^{22,23}. We recently attempted to explore the contributions of proteostasis to genomic responses associated with cell cycle phases in response to E2. For this, we employed various chemical/pharmacological agents, alone or in combinations, to enrich cell cycle phases in breast adenocarcinoma-derived E2-responsive and ER α -synthesizing MCF7 and T47D cells that display distinct molecular characteristics and cycle progression profiles^{24–28}. However, we obtained results with reproducibility and reliability issues that limited the utility of some of these approaches.

Among approaches, withdrawal of estrogen from cell culture environments that primarily rely on dextran-coated charcoal (CD) treatment of fetal bovine serum (FBS), CD-FBS, as the main component of tissue culture media has been used, as we have^{22,23}, as an effective mean for cell cycle synchronization of cell models derived from breast adenocarcinomas^{29–37}. Subsequent supplementation of synchronized cells with estrogen alone or together with chemical/pharmacological agents has provided experimental models for specific cell cycle phase enrichments. However, various factors including the preparation and use of CD-FBS, as well as the nature, concentration, and duration of chemical/pharmacological agents in cycle synchronizations also generate experimental variability undermining reproducibility^{35,38}.

We here wanted to reassess cell cycle synchronization-based phase enrichment approaches with CD-FBS alone or in combination with chemical/pharmacological agents in MCF7 and T47D cells to provide a standardizable framework for cell cycle studies. We also used, without or with CD-FBS, the double thymidine block approach as a widely utilized chemical cell cycle synchronization technique that relies on the inhibition of DNA synthesis by excess thymidine to arrest cells at the G1/S boundary before DNA replication^{39–42} for comparative analysis. We find here that the maintenance of MCF7 or T47D cells in CD-FBS containing growth medium effectively synchronizes cells at the G0/G1 phase. We also find in MCF7 cells that supplementation of CD-FBS with E2 enriches the S phase population and together with nocodazole and nocodazole-coupled mitotic shake-off augments the population in the G2/M phase, respectively. On the other hand, the double thymidine block with nocodazole or nocodazole-coupled mitotic shake-off is an effective approach to obtain enriched S and G2/M phase populations of T47D cells.

Materials and methods

Reagents

17 β -estradiol (E2; Cat # E2257), 4-hydroxytamoxifen (4-HTam; Cat # H7904) as the active metabolite of tamoxifen, thymidine (Cat # T1895), and propidium iodide (Cat # P4170) were purchased from Sigma-Aldrich (MO, USA). Imperial Chemical Industries 182,780, (ICI, Cat # 1047), as well as aphidicolin (Cat # 5736) and 2,3-DCPE (Cat # 2137), were obtained from BioTechnie-Tocris (Bristol, UK). Antibodies for ER α (Cat # sc-543), Cyclin E (Cat # sc-247), and HDAC1 (Cat # sc-81598) were obtained from Santa Cruz Biotechnology (SCBT, Santa Cruz, CA, USA), and the antibody for Cyclin B1 (Cat # 554176) was obtained from BD Biosciences (NJ, USA). We purchased an antibody for Ki-67 (Cat # RM-9106-S0) and RNase A (Cat # EN0531) from Thermo Fisher Scientific (Waltham, MA, USA). Goat anti-rabbit (Cat # R-05072) and goat anti-mouse (Cat # R-05071) secondary antibodies conjugated with horseradish peroxidase were obtained from Advanta Inc., and the Alexa Fluor-488 Goat anti-mouse secondary antibody (Cat # 405319) was obtained from BioLegend (CA, USA). Triton X-100 (Cat # A4975) was purchased from AppliChem, Germany.

Pageruler Prestained Protein Ladder (ThermoFisher, Cat # 26616) or Pageruler Plus Prestained Protein Ladder (ThermoFisher, Cat # 26619) was used as the molecular mass marker.

E2 or ICI was dissolved in Ethanol (Sigma-Aldrich, Cat # 1.00983) to 10^{−3} M as the stock concentration, whereas 4-HTam was dissolved in DMSO (AppliChem, Cat # A3672) to 5 × 10^{−2} M as the stock concentration and kept at −20°C.

Cell lines and growth conditions

a. Cell growth. We assessed the cell cycle enrichment of MCF7 and T47D cells from ATCC (American Type Culture Collection, VA, USA) as E2-responsive and ER α -synthesizing cell models for cycle synchronization studies, as we described previously^{23,43}. MCF7 cells were maintained in Dulbecco's Modified Eagle Medium (DMEM) without phenol red (Sartorius, Cat # 01-053-1 A, Israel) containing high glucose (4.5 g/L) supplemented with 10% fetal bovine serum (FBS, Sartorius, Cat # 04-007-1 A), 1% penicillin-streptomycin (Sartorius, Cat # 03-031-1B) and 1.2% L-glutamine (Sartorius, Cat # 03-020-1B). For the maintenance of T47D cells, we used the Roswell Park Memorial Institute (RPMI) 1640 medium without phenol red (Sartorius, Cat # 01-103-1 A) supplemented with 10% FBS, 1% penicillin-streptomycin and 1.2% L-glutamine. Media of cultured cells incubated in a humidified incubator with 5% CO₂ at 37 °C were refreshed every three days. Cells were passaged for a maximum of eight passages. Cells were routinely subjected to mycoplasma testing with PCR using MycoAlert Mycoplasma Detection Kit (Lonza, Cat # LT07-318, Switzerland).

Addressing the mitogenic effects of steroid hormones including estrogens requires minimizing their effects on cellular growth. This is primarily accomplished with approaches using hormone withdrawal by the use of CD treatment of FBS. However, the presence of residual estrogens and estrogen-like compounds in cell culture systems can also affect cell proliferation. One concern is centered around the presence of phenol red in tissue culture media. Phenol red, which is the standard pH indicator in various cell and tissue culture media, was earlier suggested to act as an, albeit weak, estrogen receptor (ER) agonist^{44,45}. Subsequent studies indicated that the relative impact of phenol red on the growth of various cell lines is associated with lipophilic impurities^{46,47} and high concentrations⁴⁸ of phenol red as well as cell culture conditions⁴⁹ and serum components of culture media⁴⁹. Therefore, it was suggested that the concentration of phenol red contaminants in current standard culture media formulations is insufficient to cause estrogenic effects⁵⁰. Consistent with this, we do not observe any estrogenic effect of phenol red on the growth of estrogen-responsive and ER-synthesizing cell lines derived from breast adenocarcinomas including MCF7 and T47D cells maintained in CD-FBS (Supplementary Information Fig. S1A & S1E). Nevertheless, the use of cell culture media without the phenol red remains the main practice among laboratories, including ours, when the effects of E2 on various cellular parameters are studied.

b. Preparation of CD-treated FBS (CD-FBS). To effectively reduce estrogens in FBS, we use a laboratory-optimized condition for the treatment of FBS twice with CD. For this procedure, we add 10 g of CD (Sigma-Aldrich, Cat # C6241) directly into a 500 ml FBS bottle and stir gently using an autoclaved magnetic stirrer bar on a stirrer for 16 h at 4 °C. We then divide CD-treated FBS into two equal aliquots in 500 ml centrifuge bottles (Nalgene; PPCO, Sigma-Aldrich, Cat # 3120-9500) to pellet CD by centrifugation at 10,800 \times g with Sorvall SLA-3000 rotor for 30 min at 4 °C. We then filter the supernatant using a low protein binding, 500 ml Vacuum Filter/Storage Bottle System with a pore size of 0.45 μ m (Corning, Cat # 430770, AZ, USA). We employ another round of treatment of this CD-FBS with 10 g CD at 4 °C for 6 h. Following centrifugation, we filter the supernatant firstly with a 500 ml Vacuum Filter/Storage Bottle System with a pore size of 0.45 μ m, then with a 500 ml Vacuum Filter/Storage Bottle System of 0.22 μ m pore size (Corning, Cat # 431097) and aliquot the filtered FBS into 50 ml aliquots for storage at -20 °C. Under these conditions, estrogen is undetectable in CD-FBS as assessed with the Elecsys Estradiol III Assay (Roche, Germany).

We functionally test each batch of CD-FBS for estrogen withdrawal using MCF7 or T47D cells. We plate MCF7 cells (2×10^5 cells/well of six-well tissue culture plates) or T47D cells (2.5×10^5 cells/well of six-well tissue culture plates) in DMEM or RPMI 1640, respectively containing 1% penicillin-streptomycin, 1.2% L-glutamine and supplemented with 10% FBS for 48 h. After 48 h, cells are washed with 1 \times PBS one time and incubated in fresh growth media supplemented with 10% CD-FBS for 72 h, a period in our hands that effectively synchronizes cells at G0/G1 (Supplementary Information; Fig. S2A & S2B), with a medium change at 48 h. Cells are then incubated in the growth medium supplemented with 10% CD-FBS without (0.01% ethanol as vehicle control) or with 10^{-9} M E2, an upper physiological level of circulating hormone in adult women⁵¹ (Supplementary Information Fig. S2C), for 24 h to assess cell cycle progression with flow cytometry, the expression of the *TFF1/pS2* gene, a well-characterized E2-ER α responsive gene^{52,53}, and the growth of cells at 72 h with media changes at 48 h (Supplementary Information Fig. S1B-S1D & S1F-S1H). We consider an effective removal of E2 from FBS if (1) E2 in comparison with the ethanol control drives cycle progression of the MCF7 or T47D cell population, (2) increases the *TFF1/pS2* expression at 24 h, and (3) augments cell growth at 72 h (Supplementary Information Fig. S1B-S1D & S1F-S1H).

c. Synchronization of cell cycles with E2 withdrawal. For the synchronization of cell cycles with CD-FBS containing growth media, MCF7 (7.5×10^5) or T47D (1×10^6) cells were plated in T-25 tissue culture flasks in DMEM or RPMI 1640 medium supplemented with 10% CD-FBS, respectively, to minimize estrogen effect for 72 h with media refreshing at 48 h. Cells were then incubated in the corresponding growth medium containing 10% CD-FBS without (0.01% ethanol, EtOH) or with 10^{-9} M E2 for three- to six-hour intervals up to 36 h to test the effects of E2 on cell cycle progression. At the termination, cells were collected with trypsinization. A portion of the collected cells was kept apart for flow cytometry and the remainder of the cells was used for western blot (WB) analysis. Cell cycle distribution was assessed with flow cytometry as described in the "Flow Cytometry" section.

d. Treatment of cells with 4-hydroxytamoxifen (4-HTam) or Imperial Chemical Industries 182,780 (ICI). To examine whether or not the growth of MCF7 or T47D cells is dependent upon E2-ER α signaling, we used selective estrogen receptor modulator 4-HTam^{54,55} or the selective estrogen receptor down-regulator ICI^{56,57} in the absence or presence of E2. Cells grown in steady state condition, that is in growth media supplemented with 10% FBS, treated without (0.0002% DMSO as the 4-HTam vehicle control or 0.01% Ethanol as the ICI vehicle control) or with various concentrations of 4-HTam or ICI for 24 h (Supplementary Information Fig. S3A & S3C). Furthermore, MCF7 or T47D cells synchronized at G0/G1 with the corresponding growth me-

dium containing 10% CD-FBS for 72 h were also treated for 24 h without (vehicle) or with 10^{-9} M E2 and/or 10^{-7} M 4-HTam or ICI (Supplementary Information Fig. S3B & S3D).

- e. **Synchronization of cell cycles with the double thymidine block (DTB) approach.** For the synchronization of cell cycles with double thymidine block, MCF7 or T47D in T-25 culture flasks were incubated in growth media containing 10% FBS and 2 mM thymidine, which was based on a concentration that was maximally effective in cell synchronization at G1/S boundary without inducing toxicity⁴², for 14 h (Supplementary Information, Fig. S4). The cells were released from thymidine treatment by twice washing the cells with 1x PBS and re-incubating them with 10% FBS containing appropriate media without thymidine for 12 h. The cells were subsequently washed and incubated with media containing 10% FBS and 2 mM thymidine for 22 h. Cells were re-released from thymidine treatment by washing the cells twice with 1x PBS and maintaining them in an appropriate media containing 10% FBS. Cells were collected with trypsinization at different time points. A fraction of the collected cells was kept apart for flow cytometry and the remainder was used for WB analysis.

To assess the effects of E2 on the DTB approach, cells grown in T-25 tissue culture flasks in media supplemented with 10% FBS for 72 h were washed twice with 1x PBS. Subsequently, cells were incubated in media containing 10% CD-FBS and 2 mM thymidine for 14 h. The cells were then released from thymidine treatment by washing cells twice with 1x PBS and incubating them in 10% CD-FBS containing appropriate media for 12 h. Cells were washed and incubated with media containing 10% CD-FBS and 2 mM thymidine for an additional 22 h. Cells were subsequently incubated in media containing 10% CD-FBS without (0.01% ethanol, EtOH as the vehicle control for E2) or with 10^{-9} M E2 for various intervals up to 32 h. Cells were collected with trypsinization at different time points. A fraction of the collected cells was kept apart for flow cytometry and the remainder of the cells was used for WB analysis.

Flow cytometry

Cells were harvested and centrifuged to eliminate dead cells for univariate analysis of cell cycle status based on total DNA content. Pelleted cells were re-suspended in 1x PBS and pelleted again. Cells were then gently re-suspended in 100 μ l of 2% CD-FBS containing PBS, fixed, and permeabilized with ice-cold 70% ethanol overnight. To prepare the cells for propidium iodide staining, the cells were pelleted to remove the ethanol. The cells were washed with ice-cold 1x PBS and pelleted. The cell pellet was re-suspended in 200 μ l of 1x PBS containing 20 μ g/ml propidium iodide, 200 μ g/ml RNase A, and 0.1% (v/v) Triton X-100 for 30 min in the dark at room temperature. Following incubation, the cells were filtered through a cell strainer (PluriSelect, Cat # 43–10040-40, Germany) to eliminate cell clumps, and then analyzed with a NovoCyte Flow Cytometer (Agilent Technologies, USA) using the B572 channel. A sample gating strategy is given in Supplementary Information, Fig. S5. In summary, after the selection of the total cell population (child population P1), single cells were selected in the SSC-H vs. SSC-A graph, yielding the child population P2. Then, the PI-H vs. PI-A graph was used to select the PI-stained population, also excluding the sub-G1 and super-G2 populations, yielding the child population P3. The child population P3 was then used in the cell cycle plot, which generates the percent distribution of the cells in each cell cycle phase. NovoExpress Software (Agilent Technologies, USA; <https://www.agilent.com/en/product/research-flow-cytometry/flow-cytometry-software/novocyte-novoexpress-software-1320805>) was used during sample acquisition and for data analysis.

For bivariate analysis of Cyclin B1 expression in conjunction with total DNA content, the collected cells were fixed overnight with ice-cold 70% ethanol, as described above. The fixed cells were pelleted and washed with 1x PBS and pelleted again. The cells were re-suspended in 500 μ l of 0.1% (v/v) Triton X-100 in 1x PBS and incubated for 20 min at room temperature. The cells were washed with 1x PBS and blocked in 1% BSA in 1x PBS for 30 min at room temperature. After the blocking, the cells were pelleted and re-suspended in 100 μ l of Cyclin B1 antibody, diluted 1:100 in 1% BSA, and incubated for 1 h at room temperature. The cells were then washed twice with 1x PBS and re-suspended in 100 μ l of Alexa Fluor-488 Goat anti-mouse secondary antibody, diluted 1:100 in 1% BSA, and incubated for 1 h in the dark at room temperature. The cells were then washed twice with 1x PBS, and re-suspended in 200 μ l of 1x PBS containing 20 μ g/ml propidium iodide and 200 μ g/ml RNase A for 30 min in the dark at room temperature. Following incubation, the cells were analyzed with a NovoCyte Flow Cytometer using the B530 channel for Alexa Fluor-488 and the B572 channel for propidium iodide. Gating was performed as described above, and NovoExpress Software was used for sample acquisition and data analyses.

Western Blot (WB)

Pelleted cells from each time point were washed twice with 1x PBS and lysed with RIPA buffer (150 mM NaCl; 5 mM EDTA, pH=8.0; 50 mM Tris, pH=8.0; 1% NP-40; 0.5% sodium deoxycholate; 0.1% SDS) containing freshly added protease (Merck, Cat # 11697498001, Germany) and phosphatase inhibitors (Merck, Cat # 4906845001). Total protein concentrations were assessed with Bradford Protein Assay (Bio-Rad, Cat # 500–0201, USA). For WB analysis, equal amounts (10 μ g) of cellular extracts were subjected to SDS-10% PAGE, as we described previously^{22,23}. It should be noted that 30 μ g protein extracts and a gradient gel (SDS 4–20% PAGE) were used for WB analyses of the Ki-67 protein. Proteins were transferred onto the PVDF (polyvinylidene difluoride) membrane (Sigma-Aldrich, Cat # 03010040001). Membranes were blocked with 0.1% TBS-T containing 5% Blotting-Grade Blocker, non-fat dry milk (Bio-Rad, Cat # 1706404), for 1 h at room temperature. Membranes were then incubated for 1 h at room temperature with the antibody specific for Cyclin B1 (1:500), Cyclin E (1:250), ER α (1:1000) or HDAC1 (1:1000) antibody (Ab) in 0.1% TBS-T, followed by the incubation at room temperature for 1 h with HRP-conjugated anti-mouse or anti-rabbit secondary antibodies (1:5000). We also used an antibody for Ki-67 (1:500; Thermo-Fisher) as a marker for proliferation. Peroxidase activity was visualized with WesternBright ECL Kit (Advanta, Cat # K-12045) using the ChemiDoc MP system (Bio-Rad) and analyzed

with Image Lab (Bio-Rad). For the quantification of protein levels in WB analyses, we used BioRad ImageLab software (<https://www.bio-rad.com/en-tr/product/image-lab-software?ID=KRE6P5E8Z>) and normalized the results with HDAC1 protein levels as the loading control.

Statistical analysis

All experiments were repeated two independent times. Results were presented as the mean \pm standard deviation (SD) using GraphPad Prism version 8.0 (<https://www.graphpad.com/>).

Results and discussion

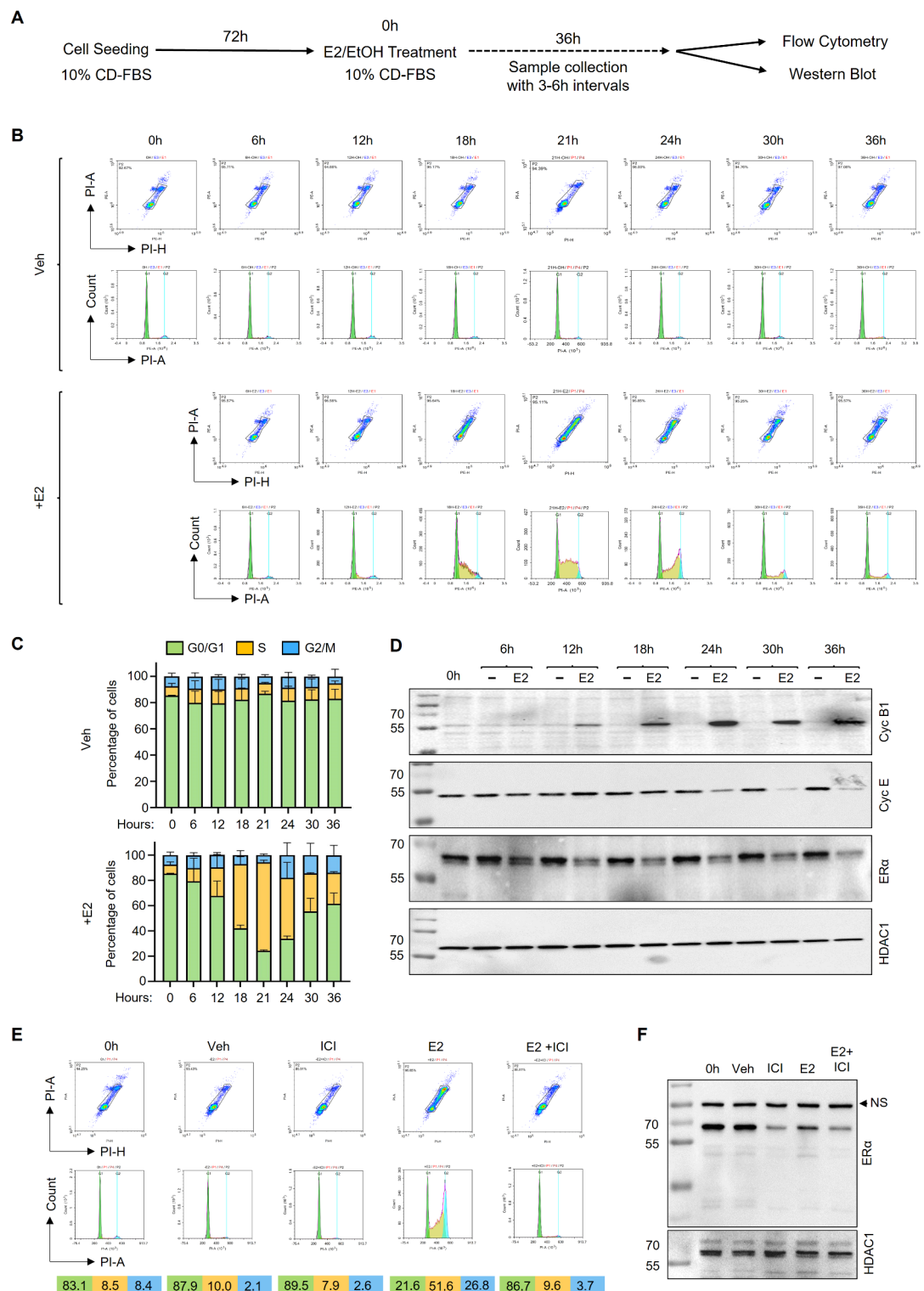
Synchronization of the cell cycle of MCF7 cells with CD-FBS with or without E2 replacement

FBS is a universal growth supplement of cell and tissue culture media required for attachment, growth, proliferation, and differentiation of human and animal cells⁵⁸. FBS is an ill-defined mixture of components containing various peptide and steroid hormones, growth factors, amino acids, proteins, vitamins, inorganic salts, carbohydrates, and antibodies as well as potential adverse factors including endotoxin, mycoplasma, and/or viral contaminants^{58–60}. The CD treatment of FBS removes a wide range of non-polar/lipophilic components, including steroid hormones^{35,61}, thereby permitting the examination of the effects of these components on cellular events in culture systems⁶². However, significant constituent variations in FBS stemming from the diversity of geographical and seasonal sources as well as from varying approaches used institutionally or commercially for the CD treatment of FBS contribute to the extent of serum component deprivation, thereby generating experimental variability and reproducibility issues^{35,58}, as we have encountered on several occasions. Based on these considerations and experiences, we employ a laboratory-optimized condition for the treatment of FBS twice with CD detailed in the Materials & Methods section and use in cell cycle synchronization studies.

To assess the effects of estrogen withdrawal on cell cycle progression, we synchronized MCF7 cells by maintaining them in DMEM containing 10% CD-FBS for 72 h (Fig. 1A). Under this condition, more than 80% of the cell population accumulates at the G0/G1 phase as assessed by flow cytometry (Fig. 1B). To examine the effects of E2 on cell cycle phase transitions, cells arrested in G0/G1 were incubated in the same medium without (0.01% ethanol, EtOH) or with 10^{-9} M E2, (also Supplementary Information, Fig. S2C), for 3–6 h intervals up to 36 h (Fig. 1A). A fraction of cells at each time point was subjected to flow cytometry while the remaining was processed for WB analysis (Fig. 1A). E2 effectively triggered cell cycle progression such that the proportion of cells in the S phase began to increase at 12 h reaching a plateau at 21 h ($65 \pm 3.5\%$) with corresponding decreases in the cell population accumulated in G0/G1 (Fig. 1B & C). At subsequent time points, cells transited to the G2 phase, completing the cycle by 30 h with an increase in G0/G1 that resulted in a desynchronized cell population at 36 h. In clear contrast, ethanol as the vehicle control did not affect cycle phase distribution as the majority of the cell population remained in the G0/G1 phase at every time-point examined.

E2-triggered cell cycle progression was reflected in changes in protein levels of Cyclin B1 or Cyclin E assessed with WB analysis (Fig. 1D; Supplementary Information, Fig. S6A). Cyclin B1 is the regulatory subunit of cyclin-dependent kinase 1 (CDK1) and is essential for the transition from the G2 phase to mitosis⁶³. On the other hand, Cyclin E as an activator of CDK2 (Cyclin-Dependent Kinase 2) is critical for the entry to and progression through the S phase⁶⁴. We observed that the protein levels of Cyclin B1 start to increase in the early S phase (at 12 h of E2 treatment) and remain elevated until the desynchronization of cells (Fig. 1D; Supplementary Information, Fig. S6A). The variation in Cyclin B1 protein levels across cell cycle phases was further confirmed with a bivariate analysis of Cyclin B1 synthesis alongside total DNA content using flow cytometry (Supplementary Information, Fig. S7 and S8). Cyclin E, on the other hand, begins to decrease at the late S phase (24 h) reaching low levels at 36 h (Fig. 1D; Supplementary Information, Fig. S6A). Previous studies showed that E2 treatment rapidly decreases ER α levels^{65–67}. Consistent with these studies, the E2 treatment of synchronized MCF7 cells reduces ER α levels to a nadir by 6 h that remains at similar levels at the remainder of the cycle as assessed with HDAC1 as the loading control (Fig. 1D; Supplementary Information, Fig. S6A). Whereas, ER α levels remain unchanged at all time points in vehicle control. Thus, E2 acts as a mitogenic factor for MCF7 cells. These results indicate that the maintenance of cells in the growth medium supplemented with CD-FBS effectively synchronizes the cell cycle of MCF7 cells culminating in an enriched G0/G1 population.

ERs also bind to various molecules with agonist, mixed agonist-antagonist, or full antagonist properties^{68,69}. Mixed agonists/antagonists, also called “selective estrogen receptor modulators” (SERMs), display distinct pharmacological effects, depending on the estrogen target tissue. Tamoxifen, TAM, as a synthetic nonsteroidal compound, for example, has been widely used for the treatment of breast cancers as an antagonist, yet it acts as an agonist in the uterus^{68,69}. Pure antagonists of estrogenic compounds, exemplified with Imperial Chemical Industries 182,780 (ICI), are steroidal analogs of estradiol, which are also referred to as the “selective estrogen receptor down-regulators” (SERDs), and act as complete antagonists^{68,69}. Most of the key amino acids in the ligand-binding cavity of ER α responsible for binding TAM and ICI are the same. However, a large side chain emanating from the core of ICI causes a significant conformational shift in the ligand binding domain of ER α that impairs dimerization and increases ER α degradation resulting in the prevention of target gene expressions^{57,70,71}. To ensure that E2-induced cell cycle progression is dependent on ER α signaling, cells synchronized at G0/G1 with the growth medium containing 10% CD-FBS for 72 h were treated for 24 h without or with 10^{-9} M E2 and/or 10^{-7} M ICI (also Supplementary Information Fig. S3D). ICI did not affect the cell population synchronized at the G0/G1 phase but it effectively blocked the E2-mediated cell cycle progression assessed with the accumulation of cells in the S phase (Fig. 1E). ICI also reduced the levels of ER α whether or not cells were treated with E2 (Fig. 1F). Thus, these observations indicate that the E2-ER α signaling is the primary pathway to induce cell cycle progression in MCF7 cells synchronized at G0/G1 in DMEM containing 10% CD-FBS for 72 h.



Synchronization of the cell cycle of MCF7 cells with the double-thymidine block (DTB) approach.

Various chemicals including lovastatin and mimosine have been used for cycle synchronization at the G1 phase. Lovastatin is a 3-hydroxy-3-methylglutaryl-coenzyme A reductase (HMG-CoA reductase) inhibitor and results in G1 cell cycle arrest by inducing CDKIs, such as p21 and p27^{72,73}. The addition of mevalonate, which increases the degradation of the CDKIs through an increased proteasome activity⁷⁴, drives the release of cells from the G1 arrest for entry into the S and G2/M phases of the cell cycle⁷⁵. Mimosine, a rare plant amino acid, reversibly arrests the progression of the cell cycle at G1 before the onset of DNA replication^{76,77}. On the other hand, double thymidine block (DTB), a widely utilized chemical technique that relies on the interruption of the deoxynucleotide metabolism pathway through competitive inhibition with excess thymidine, arrests cells at the G1/S boundary before DNA replication³⁹⁻⁴².

◀Fig. 1. Effects of 17β estradiol (E2) on cell cycle progression of MCF7 cells synchronized at G0/G1 by hormone withdrawal. (A–F) MCF7 cells were plated and grown in DMEM medium supplemented with 10% CD-FBS for 72 h with media change at 48 h. (A–D) Cells were subsequently maintained in the same medium containing 0.01% ethanol (EtOH) as vehicle control or 10^{-9} M E2 for 3–6 h intervals up to 36 h. At the termination, cells were collected with trypsinization. (B) A fraction of cells was subjected to the flow cytometry analysis (C) represented with a bar graph of two independent replicates, and (D) the remaining fraction was processed for WB analysis using an antibody for Cyclin B1 (Cyc B1), Cyclin E (Cyc E), ER α , or HDAC1. Molecular masses in kDa are indicated. (E & F) MCF7 cells synchronized at G0/G1 by the CD-FBS approach (0 h) were treated without (0.01% EtOH) or with 10^{-9} M E2 and/or 10^{-7} M ICI for 24 h. Cells were collected with trypsinization and (E) subjected to the flow cytometry analysis or (F) WB using an antibody for ER α or HDAC1. In B & D and E & F, representative images from the same experiment conducted two independent times are shown. G0/G1, S, and G2/M indicate cell cycle phases. NS indicates a nonspecific protein species detected with the ER α antibody.

Based on variable results with lovastatin and mimosine in our earlier explorations, we selected to use a DTB approach⁴² to synchronize MCF7 cells as an alternative method to the CD-FBS treatment. To assess the effects of DTB, MCF7 cells grown in DMEM containing 10% FBS were subjected to DTB with an initial 2 mM thymidine treatment for 14 h followed by a release from thymidine for 12 h and re-blocking with 2 mM thymidine for 22 h (Fig. 2A). The DTB approach synchronized MCF7 cells at the G1/S border with a substantial population of cells also present at the beginning of the S phase, as reported previously⁷⁸, independently of thymidine concentrations we tested (2–10 mM) (Fig. 2B and C; Supplementary Information, Fig. S4A). Nevertheless, the release from DTB (RDTB) rapidly, within 6 h, drove the progression of cells through the S phase: Cells transitioned to G2 at 8 h after the release from DTB and subsequently desynchronized at 14 h (Fig. 2B and C). The cycle phase transitions were also reflected in high levels of Cyclin E at the beginning of the release of DTB which started to decline in the late S phase reaching steady-state levels until the desynchronization of cells. The levels of Cyclin B1, on the other hand, began to increase at the progression of the S phase and sharply declined thereafter at levels similar to those observed with unsynchronized cells; whereas, ER α levels remained primarily unchanged throughout the cycle as the protein levels of HDAC1, which was used as the loading control (Fig. 2D; Supplementary Information, Fig. S6B).

To examine whether or not the accumulation of cells at the G1/S transition as well as cell cycle progression following the release of DTB requires the presence of E2, we assessed the combination of DTB and CD-FBS on cell cycle synchronization. For this, MCF7 cells maintained in DMEM containing 10% FBS for 72 h were washed and incubated in DMEM supplemented with 10% CD-FBS containing 2 mM thymidine for 14 h. Cells were subsequently released from the thymidine block with DMEM containing 10% CD-FBS for 12 h. Cells were re-incubated with DMEM medium containing 10% CD-FBS and 2 mM thymidine for 22 h. For the release, cells were treated without (0.01% EtOH) or with 10^{-9} M E2 in DMEM containing 10% CD-FBS for 2-to-4 h intervals up to 32 h (Fig. 3A). This approach effectively synchronized the cells in G0/G1 as more than 80% of the cell population accumulated in the G0/G1 phase at the time of the release (0 h) from the DTB (Fig. 3B and C) as similarly observed with the CD-FBS treatment (Fig. 1B and C). Following the DTB release, the presence of E2 triggered cell cycle progression, although with a substantial delay compared to DTB alone but similar to those observed with the CD-FBS approach. We observed that E2 treatment-coupled DTB release initiated the cell cycle progression with cells entering the S phase by 12 h, reaching a maximal population by 20 h, and exiting the S phase by 24 h with eventual desynchronization of the cycle at 32 h (Fig. 3B and C). Cell cycle progression was correlated with Cyclin B1 levels, which showed an increase at the beginning of the S phase and remained at high levels thereafter. In contrast, protein levels of Cyclin E declined with the S phase. ER α levels also decreased upon E2-triggered cell cycle progression without altering levels of HDAC1, which was used as the loading control (Fig. 3D; Supplementary Information, Fig. S6C).

To ensure that E2 treatment-coupled DTB release is dependent on ER α signaling, cells synchronized at G0/G1 with the DTB approach in the growth medium containing 10% CD-FBS were treated for 24 h without or with 10^{-9} M E2 and/or 10^{-7} M ICI at the time of release. ICI did not affect the G0/G1 phase population, but it effectively blocked the cycle progression assessed with the accumulation of cells in the S phase induced by E2 (Fig. 3E). ICI also reduced the levels of ER α whether or not cells were treated with E2 (Fig. 3F). Thus, the E2-ER α signaling is the primary factor in driving cell cycle progression in MCF7 cells synchronized at G0/G1 with CD-FBS alone or in combination with DTB.

Synchronization of cell cycle with antiestrogens in MCF7 cells.

Antiestrogens including 4-HTam and ICI block the cycle of MCF7 cells^{31,37,79–81} and the block can be reversed by E2 resulting in a synchronized cohort of cells progressing through the S phase³¹. This raises the possibility that the withdrawal of antiestrogens could drive cell cycle progression blocked at G0/G1 of cells maintained in the complete growth medium. This approach could generate a simplified experimental model necessitating the use of only antiestrogens for the synchronization of MCF7 cells. To assess this possibility, we treated unsynchronized MCF7 cells maintained in DMEM medium containing 10% FBS without or with 10^{-7} M 4-HTam or ICI (Supplementary Information, Fig. S3) for 48 h, the duration of which was based on our observations that MCF7 cells complete cell cycle within 36 h (Fig. 1B). Both compounds effectively synchronized MCF7 cells at the G0/G1 phase (Fig. 4A and D). Nevertheless, the treatment of cells with ICI was more effective in accumulating cells at G0/G1 (% 84 ± 1.5) compared to the 4-HTam treatment (% 72 ± 3). The release from the block by incubating cells in the fresh growth medium without 4-HTam or ICI (post-release, PR) for up to 72 h did not allow cells to

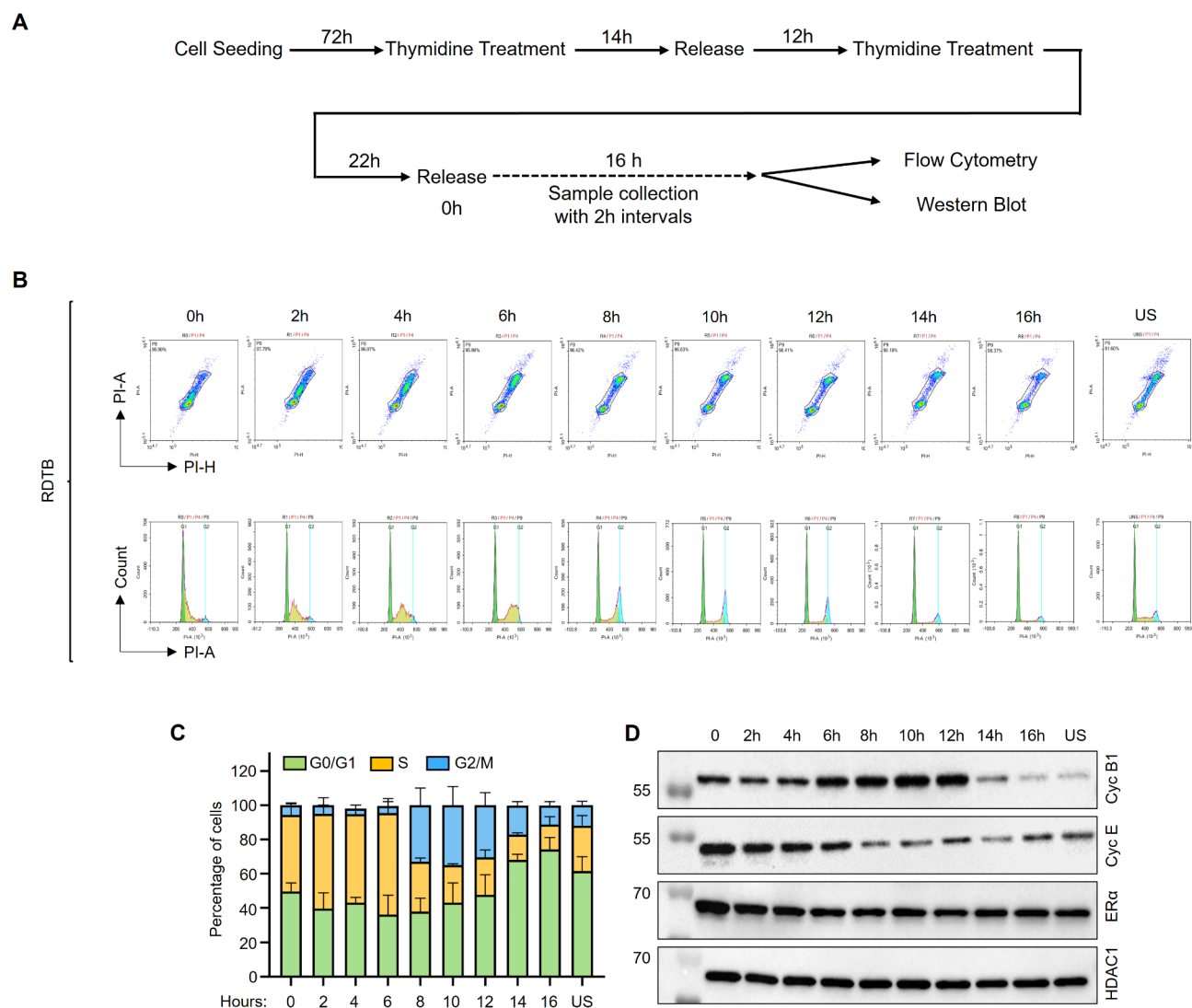


Fig. 2. Cell cycle progression following the release of synchronized MCF7 cells from double thymidine block. **(A–D)** MCF7 cells maintained in DMEM medium supplemented with 10% FBS were incubated in the same medium containing 2 mM thymidine for 14 h. Cells were then released from thymidine treatment by twice washing the cells with 1x PBS and re-incubating them in DMEM medium containing 10% FBS without thymidine for 12 h. Cells were subsequently washed and incubated with the same medium containing 2 mM thymidine for 22 h. Cells were released from the double thymidine block (RDTB) by freshening the culture medium (0 h). Cells were collected with trypsinization at 2 h intervals for 16 h following release and **(B)** subjected to flow cytometry analysis **(C)** with the result of two independent experiments represented with a bar graph. **(D)** Cells were also prepared for and subjected to WB using antibodies for Cyclin B1 (Cyc B1), Cyclin E (Cyc E), ER α , or HDAC1. Molecular masses in kDa are indicated. In **B** & **D**, representative images from the same experiment replicated two independent times are presented. G0/G1, S, and G2/M indicate cell cycle phases. US indicates unsynchronized cells.

transit cycle phases. We observed that cells synchronized at G0/G1 by the 10^{-7} M 4-HTam treatment for 48 h remained at G0/G1 at which the percentage of cells increased in a time-dependent manner without alteration in ER α levels (Fig. 4B). Instead, the percentage of 10^{-7} M ICI pre-treated cells accumulated at G0/G1 at 24 h remained the same throughout the experimental period (Fig. 4D). ICI pre-treatment, as expected, reduced ER α levels as assessed with WB (Fig. 4E). A previous study suggested that ICI-mediated cycle arrest of MCF7 cells at G0/G1 have characteristics of G0 rather than the G1 phase⁸². Ki67, also known as the Marker of Proliferation Ki-67 (MKI67), is strictly associated with cell proliferation. Ki67 protein is present during all active phases of the cell cycle (G1, S, G2, and M), but is absent from resting cells (G0)^{83,84}. This stage-specific synthesis of Ki67 has been used as a marker for active cell proliferation^{83,84}. WB analysis of MCF7 cells pre-treated with ICI using an antibody specific to Ki67 as a marker for proliferation revealed that Ki67 synthesis is indeed undetectable compared to unsynchronized vehicle-treated control cells (Fig. 4F). On the other hand, Ki67 levels in 4-HTam pre-treated MCF7 cells showed a time-dependent decline that was inversely correlated with an increase in the

percentage of cells accumulated in G0/G1 throughout the experimental duration (Fig. 4C). Thus, as suggested previously for ICI⁸², antagonist treatment of exponentially growing MCF7 cells in complete medium results in a quiescent state of cells unresponsive to the removal of the compound.

Enrichment of cell cycle phases by E2 treatment-coupled chemical agents in MCF7 cells

Based on our results that CD-FBS effectively synchronizes MCF7 cells in G0/G1 and the replacement of E2 efficiently drives cycle progressions, we wanted to assess whether or not we could also obtain cell populations enriched specifically at S, G2, and/or M phases with various chemical agents. Aphidicolin, a tetracyclic diterpenoid, reversibly inhibits functions of DNA polymerase α , δ , and ϵ arresting cell cycle progression at the G1/S transition thereby blocking DNA synthesis in cells that have entered S-phase⁸⁵. We, therefore, reasoned that the co-treatment of E2-treated cells with aphidicolin could enrich the population in the S phase dependent upon the duration of E2 treatment. To test this prediction, we used 10 μ M of aphidicolin at different time points of the S phase following the E2 treatment of MCF7 cells synchronized at G0/G1. We observed no significant effect of aphidicolin at this, or other concentrations (Supplementary Information, Fig. S9A) on the S phase population at any point we tested (Supplementary Information, Fig. S9B & S9C). Similarly, 20 μ M, based on preliminary studies (Supplementary Information, Fig. S10A), 2,3-DCPE, a synthetic compound suggested to induce S phase arrest by activating the ATM/ATR-Chk1-Cdc25A signaling pathway in DLD-1 colon cancer cells^{86,87}, did not further enrich the S phase population of MCF7 cells generated by E2 treatment (Supplementary Information, Fig. S10B).

These results suggest that harvesting cells at a specific time point corresponding to the highest population of MCF7 cells accumulated in the S phase, the 21 h E2 treatment as our results suggest, is the best option for the S phase enrichment.

Despite the effective synchronization by CD-FBS and subsequent progression through cycle phases by E2 treatment of MCF7 cells, the rapid progression through the G2/M phase for the cycle completion does not generate a significantly enriched cell population at the G2/M phase. Nocodazole is an anti-mitotic agent that reversibly interferes with the polymerization of microtubules by binding to β -tubulin⁸⁸. This binding impairs the formation of the metaphase spindles during the cell division cycle, thereby arresting cells in G2/M leading to the prevention of mitosis⁸⁸. Nocodazole-treated cells can also be harvested by mitotic shake-off to generate a high percentage of cells at the M phase. Mitotic shake-off exploits the decreased membrane surface area of spherical mitotic cells attached to the culture plate thereby allowing the detachment of cells by gentle shaking⁸⁹. To enrich the G2/M population, we treated MCF7 cells synchronized at G0/G1 by the CD-FBS approach with 10^{-9} M E2 for varying durations to enrich the cell population in different stages (entrance, accumulation, and exit) of the S phase (Fig. 5A; Supplementary Information, Fig. S11). Cells were then subjected to various concentrations (0.3 to 1.2 μ M) of nocodazole for 6 h in the absence or presence of E2. We observed that 0.3 μ M nocodazole, as the minimal concentration, at 21 h of E2 treatment further enriched the G2/M phase population (Fig. 5B and E). Moreover, we obtained a nearly pure population of cells ($\geq 90\%$) in the G/M phase by nocodazole-coupled mitotic shake-off (Fig. 5C). It should be cautioned that the size of the G2/M phase population obtained with mitotic shake-off is substantially lower compared to other phases. When a large G2/M population is needed, a large-scale initial experimental setup may be suggested.

Thus, nocodazole alone or nocodazole-coupled mitotic shake-off could be used for the enrichment of the G2/M phase of the cell cycle induced by E2 in MCF7 cells.

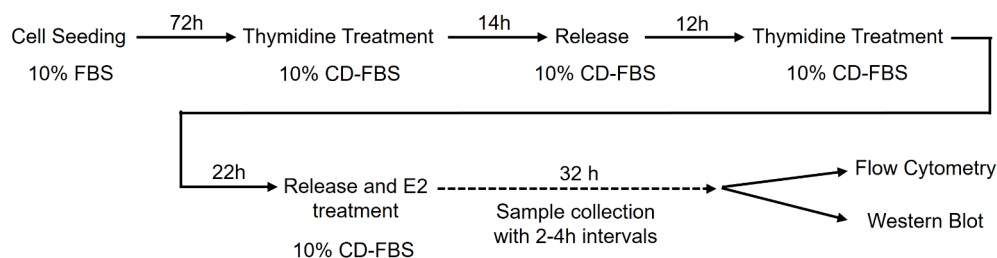
Enrichment of cell cycle phases using various approaches in T47D cells.

Although MCF7 and T47D cells are derived from a metastatic site of pleural effusion, they display distinct molecular characteristics and cell cycle profiles^{24–28}. We, therefore, wanted to assess whether or not T47D cells could be synchronized, and cycle phase enriched with approaches we employed for MCF7 cells. To examine the effectiveness of the CD-FBS approach on cell cycle synchronization of T47D cells, cells grown in RPMI 1640 supplemented with 10% CD-FBS for 72 h were treated without (0.01% EtOH) or with 10^{-9} M E2 for 6 h intervals up to 36 h. As we observed with MCF7 cells, CD-FBS synchronized T47D cells efficiently in the G0/G1 phase. The supplementation of the medium with 10^{-9} M E2 induced cycle progression of T47D cells in a time-dependent manner. However, E2 drove only a small fraction of the G1 phase population into cycle progression such that the maximal percentage of cell population accumulated in the S phase at 24 h was less than 25%. The S phase cell population subsequently traversed to G2 and desynchronized at 36 h (Fig. 6A and B). These phase transitions were correlated with the levels of Cyclin E and B1 assessed with WB. E2 treatment of cells rapidly reduced ER α levels which remained at low levels in contrast to HDAC1, used as the loading control, with levels similar throughout the cell cycle (Fig. 6C; Supplementary Information, Fig. S6D). E2 effects on cell cycle progression were ER α -mediated because ICI prevented the accumulation of cells in the S phase at 24 h (Fig. 6D) and decreased ER α levels without or with E2 (Fig. 6E).

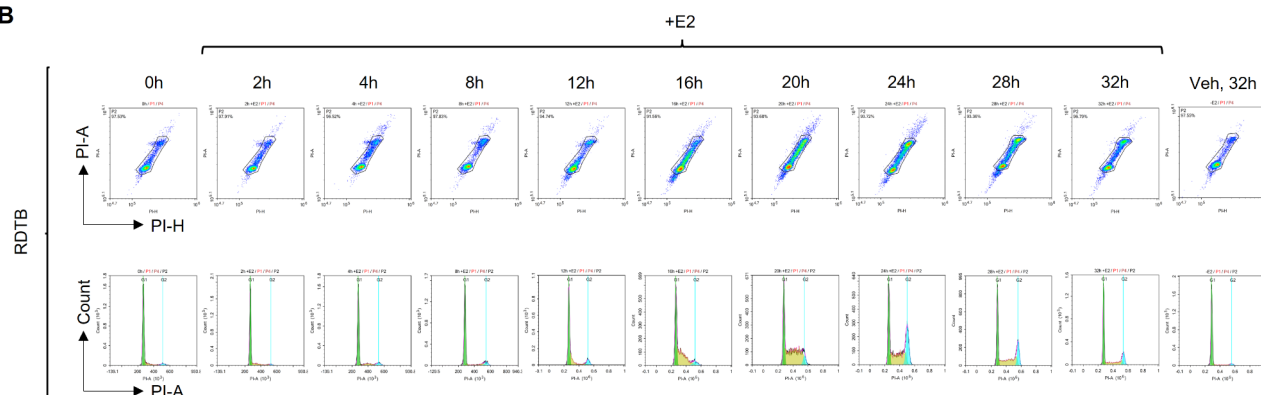
Synchronization of T47D cells grown in RPMI 1640 supplemented with 10% CD-FBS by the identical DTB approach employed for MCF7 cells partially synchronized T47D cells at the G1 phase (0 h) with a substantial cell population ($29 \pm 1.8\%$) present at the G1/S transition (Fig. 7A and B). The release from DTB with a concomitant supplementation of the medium with 10^{-9} M E2 led to cells accumulated at G1 and/or G1/S transition progress through cycle phases which were completed at 12 h (Fig. 7A and B), as reflected in varying levels of Cyclin E, Cyclin B1, and ER α in the presence of E2 by WB analyses (Fig. 7C).

Thus, it appears that although E2-ER α signaling contributes to cell cycle progression, it is not sufficient to drive the large population of cells synchronized with DTB in the growth medium supplemented with CD-FBS to transit through cell cycle phases. This, in turn, suggests that in addition to estrogens, CD treatment of FBS also removes components critical for T47D cell proliferation. To test this possibility, we employed the DTB approach on T47D cells grown in RPMI 1640 medium supplemented with 10% FBS. We indeed observed that

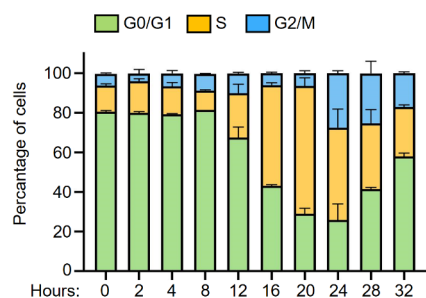
A



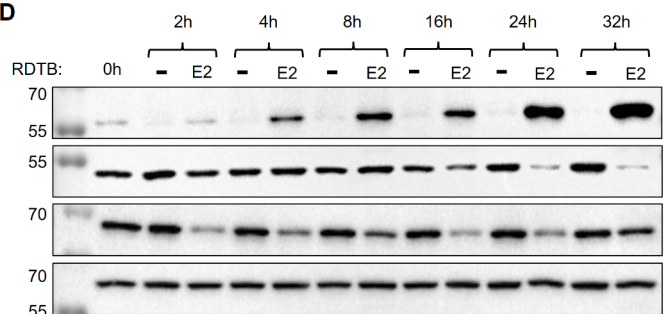
B



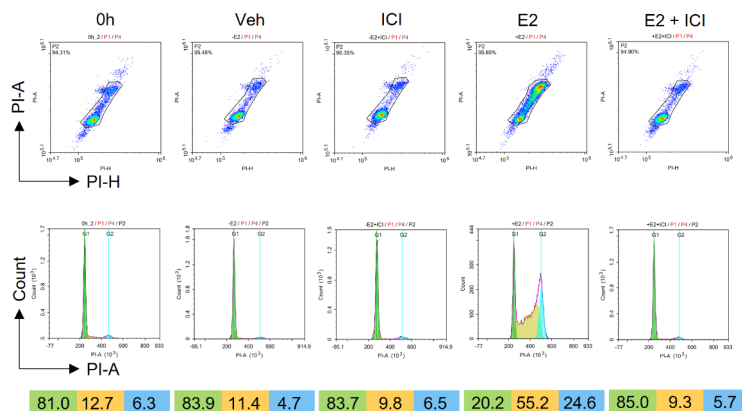
C



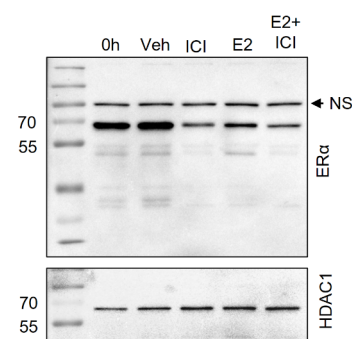
D



E



F



DTB partially synchronized the cells at G1 (0 h) and the G1/S transition with a substantially higher percentage ($45 \pm 1.5\%$) of cells compared to that observed with the DTB together with the CD-FBS approach ($29 \pm 2\%$) (Fig. 8A and B). The withdrawal of DTB effectively mirrored T47D cells accumulated at G1 and G1/S to transit cell cycle phases within 12 h with Cyclin B1 levels mirroring cycle phase transitions without affecting the levels of ERα (Fig. 8C; Supplementary Information, Fig. S6E).

Thus, while the CD-FBS approach effectively synchronizes T47D cells at the G0/G1 phase, E2 alone is insufficient to drive the large population of cells accumulated at G0/G1 to transit through phases for cycle completion. On the other hand, CD-FBS supplemented with E2 and DTB partially synchronizes cells at G1 with a large population of cells remaining at the G1/S transition in a manner observed with DTB alone. Nevertheless, the enrichment of the S phase population could be achieved following the release of the cells from DTB alone.

Fig. 3. Effects of 17β estradiol (E2) on cell cycle progression of MCF7 cells synchronized at G0/G1 by hormone withdrawal and double thymidine block. (A–F) MCF7 cells grown in DMEM medium supplemented with 10% FBS in T-25 tissue culture flasks for 72 h were washed and incubated in the fresh medium containing 10% CD-FBS together with 2 mM thymidine for 14 h. Cells were then released from thymidine treatment by washing the cells with 1x PBS and re-incubating them in DMEM medium containing 10% CD-FBS without thymidine for 12 h. Cells were subsequently washed and incubated with DMEM medium containing 10% CD-FBS and 2 mM thymidine for an additional 22 h. Cells were released from the double thymidine block (RDTB) by washing the cells and incubating them with DMEM medium containing 10% CD-FBS in the absence (0.01% EtOH) or presence of 10^{-9} M E2 for 2–4 h intervals up to 32 h. At the termination at each time point, cells were collected with trypsinization. (B) A fraction of cells was subjected to flow cytometry analysis (C) with a bar graph representing the results of two independent experiments. G0/G1, S, and G2/M indicate cell cycle phases, and (D) the remaining fraction of cells was processed for WB using an antibody for Cyclin B1 (Cyc B1), Cyclin E (Cyc E), ER α , or HDAC1. (E & F) MCF7 cells synchronized at G0/G1 by CD-FBS and double thymidine block were treated without (0.01% vehicle) or with 10^{-9} M E2 and/or 10^{-7} M ICI for 24 h. (E) Cells were collected with trypsinization and subjected to the flow cytometry analysis or (F) WB using an antibody for ER α or HDAC1. In E & F, representative images from the same experiment are shown. G0/G1, S, and G2/M indicate cell cycle phases. NS designates a nonspecific protein species detected with the ER α antibody. Molecular masses in kDa are indicated.

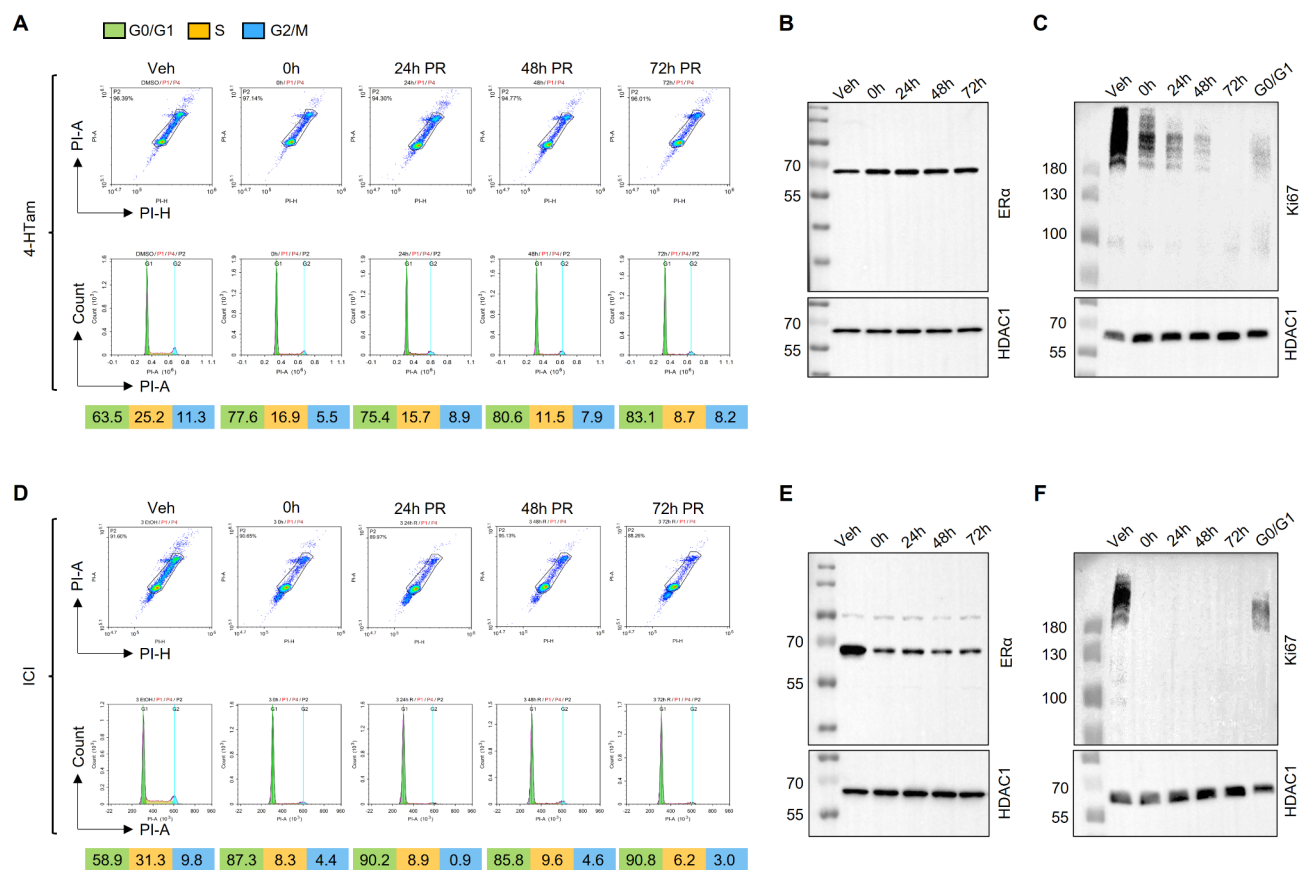


Fig. 4. Effects of 4-Hydroxytamoxifen, 4-HTam, or Imperial Chemical Industries 182,780, ICI, on the synchronization and progression of cycle phases of MCF7 cells. (A–F) MCF7 cells maintained in DMEM medium supplemented with 10% FBS were incubated in fresh media containing 0.0002% DMSO or 0.01% EtOH as vehicle control or (A–C) 10^{-7} M 4-HTam or (D–F) ICI respectively for 24 h. Cells were washed with 1x PBS and either immediately collected (0 h) by trypsinization or maintained in DMEM medium supplemented with 10% FBS (post-release, PR) at 24 h intervals for 72 h with a medium change at 48 h and subsequently collected by trypsinization. (A & D) A fraction of collected cells was subjected to flow cytometry analysis, and (B & C and E & F) the remaining cells were subjected to WB using an antibody specific for ER α , HDAC1, or Ki67. Molecular masses in kDa are indicated. G0/G1, S, and G2/M indicate cell cycle phases. Representative images from the same experiment replicated two independent times are shown.

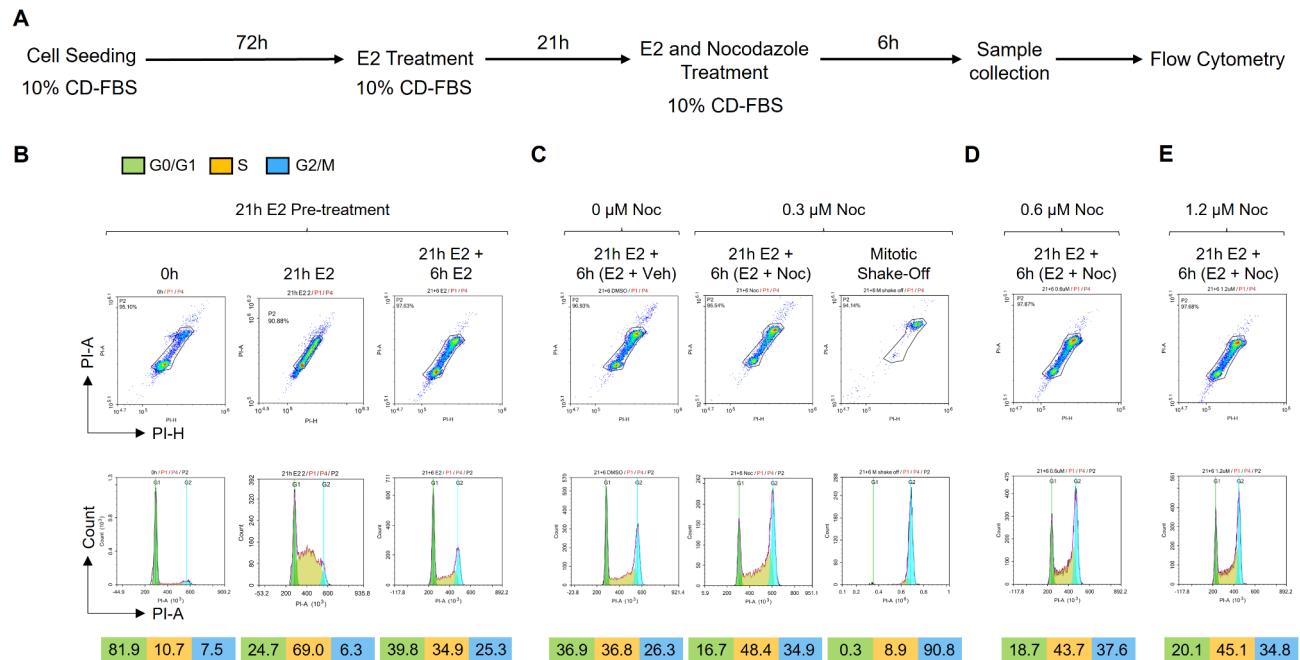


Fig. 5. Effects of various concentrations of nocodazole (Noc) on the G2/M phase in synchronized MCF7 cells progressed to the S phase in response to the E2 treatment. (A–E) MCF7 cells were grown in DMEM medium supplemented with 10% CD-FBS for 72 h. Cells were either collected by trypsinization (0 h) or treated in the same medium with 10^{-9} M E2 for 21 h. Cells were then washed and incubated in the same medium containing (B) 10^{-9} M E2 (C) and/or 0 (Veh), 0.3, (D) 0.6 or (E) 1.2 μ M nocodazole (Noc) for an additional 6 h. Cells were either subjected to trypsinization or mitotic shake-off for collection and subjected to flow cytometry. Representative images with cell cycle phases from the same experiment conducted two independent times are presented.

We also examined whether we could further enrich the G2/M phase population with the nocodazole treatment of T47D cells synchronized with DTB. We treated T47D cells at 2 h of DTB release (Fig. 8D), which was based on the preliminary studies in which 2 h post-DTB release was the optimal time for nocodazole to enrich cells in G2/M in 6 h (Supplementary Information, Fig. S12). We observed that nocodazole compared with vehicle control (DMSO) enriches the G2/M phase population (Fig. 8E). Furthermore, nocodazole-coupled mitotic shake-off yielded a nearly pure G2/M phase population ($\geq 90\%$) (Fig. 8E). Thus, as with MCF7 cells, nocodazole alone or together with mitotic shake-off can be used for the enrichment of the G2/M phase in synchronized T47D cells.

Conclusion

Cell cycle activation and re-entry are fundamental processes that underpin cellular proliferation, enabling cells to divide and propagate^{90,91}. The regulation of the cell cycle is tightly controlled by checkpoints located at key phases, including G1, G2/M, and the spindle assembly. These checkpoints serve as critical surveillance mechanisms to preserve genomic integrity by ensuring proper DNA replication, damage repair, and chromosome segregation^{90,91}. Deregulation of checkpoints often results in the development of various disorders, including cancer. However, these disruptions also create unique vulnerabilities that can be exploited for therapeutic purposes^{90,91}. Pharmacological interventions that target key regulatory molecules within specific cell cycle phases have emerged as a promising strategy in anticancer drug development. These treatments disrupt the normal progression of the cycle, thereby halting the proliferation of cancer cells^{92,93}. DNA-damaging agents, another cornerstone of cancer therapy, act by compromising the genomic integrity of cancer cells leading to cell death or inhibition of cellular growth, further enhancing their therapeutic potential^{94,95}. Despite these advances, the dynamic and adaptable nature of the cell cycle often facilitates the development of drug resistance, posing significant challenges to effective treatment. Cancer cells can exploit the plasticity of the cell cycle to evade the cytotoxic effects of therapies, necessitating the development of innovative treatment strategies. A more comprehensive understanding of the interplay among cell cycle regulation, anticancer agents, and resistance mechanisms holds great promise for advancing therapeutic approaches including drug repurposing, which involves repositioning existing medications for new clinical applications^{96,97}. Such strategies can effectively target actively dividing cancer cells while overcoming cellular adaptations that contribute to resistance^{98,99}.

As with other tissue cancers, breast cancer comprises a heterogeneous group of tumors displaying dramatic variations in clinical presentation, morphology, molecular features, biological behavior, and response to therapy^{100–102}. Breast cancer is categorized into clinical subtypes primarily by receptor expression statuses^{100–102}. ERα is a predominant endocrine regulatory protein in the breast tissue and in estrogen-induced breast cancer

that accounts for more than 70% of cases. The current modalities for the treatment of ER-positive breast cancer are centered on agents with diverse pharmacology to reduce/ablate the circulating estrogens or to alter/prevent ER function. Approaches to perturb the estrogen signaling are usually successful in the remission of established tumors. However, many breast tumors eventually develop resistance to endocrine therapies^{6,103}.

Despite being prone to genetic and phenotypic alterations due to growth conditions and the evolution of clonal populations over time^{24,25,104,105}, breast cancer cell lines have been invaluable in vitro model systems for gaining mechanistic insight into cellular phenotype, drug discovery, and resistance. Of a large number of E2-responsive ER α -synthesizing breast cancer cell lines with distinct features^{25,28,106}, MCF7 and T47D cells have been widely used for a better understanding of integrated molecular events that coordinate cellular proliferation in response to the E2-ER α signaling. Our previous attempts to delineate the contribution of proteostasis to genomic events mediated by the E2-ER α signaling in cycle phase enriched populations of synchronized MCF7 or T47D cells with various chemical/pharmacological agents yielded variable and unreliable results. We, therefore, reassessed cell cycle synchronization-coupled phase enrichment with CD-FBS alone or in combination with chemical/pharmacological agents in MCF7 and T47D cells.

Based on our results, we conclude that the maintenance of MCF7 cells in the growth medium supplemented with 10% CD-FBS and subsequent progression of cell cycle phases with the supplementation with E2 of the same growth medium is the most effective approach for cell cycle synchronization and synchronization-coupled cycle phase enrichment. MCF7 cells maintained in CD-FBS containing growth medium for 72 h accumulate effectively in the G0/G1 phase. The treatment of MCF7 cells synchronized at G0/G1 with E2 for 21 h leads to the S phase enrichment. Nocodazole treatment of MCF7 cells at the S phase following 21 h of E2 treatment for 6 h augments the G2/M phase population; whereas, nocodazole-coupled mitotic shake-off yields a nearly pure population in the G2/M phase. Overall, our results indicate that E2 is mitogenic for MCF7 cells and E2-ER α signaling is the primary pathway that drives cell cycle progression in MCF7 cells synchronized at G0/G1 using CD-FBS alone or in combination with DTB.

Similarly, the CD-FBS approach effectively synchronizes T47D cells at G0/G1 and the E2 treatment induces cycle phase transitions. However, a small population of cells, in contrast to MCF7 cells, accumulated in G0/G1 progresses through cycle phases in response to E2, rendering the enrichment of S and/or G2/M phases with the CD-FBS approach difficult. This suggests that other serum factors alongside estrogens removed by the CD treatment critically contribute to the proliferation of T47D cells. The DTB approach increases the cell population in the S phase at 2 h of release following DTB whether or not cells are maintained in CD-FBS. However, the presence of a substantial population at the early S phase following the release of cells from DTB poses challenges for the G1 enrichment, which may require other approaches. Nevertheless, nocodazole alone or together with mitotic shake-off can be used for the enrichment of the G2/M phase of T47D cells synchronized with the DTB approach.

While our results may offer a framework for cell cycle synchronizations and synchronization-coupled cell cycle phase enrichments of MCF7 and T47D cells, they are also a reminder that cell lines with remarkably distinct phenotypic features may require tailored approaches and protocols for the enrichment of cell cycle phases.

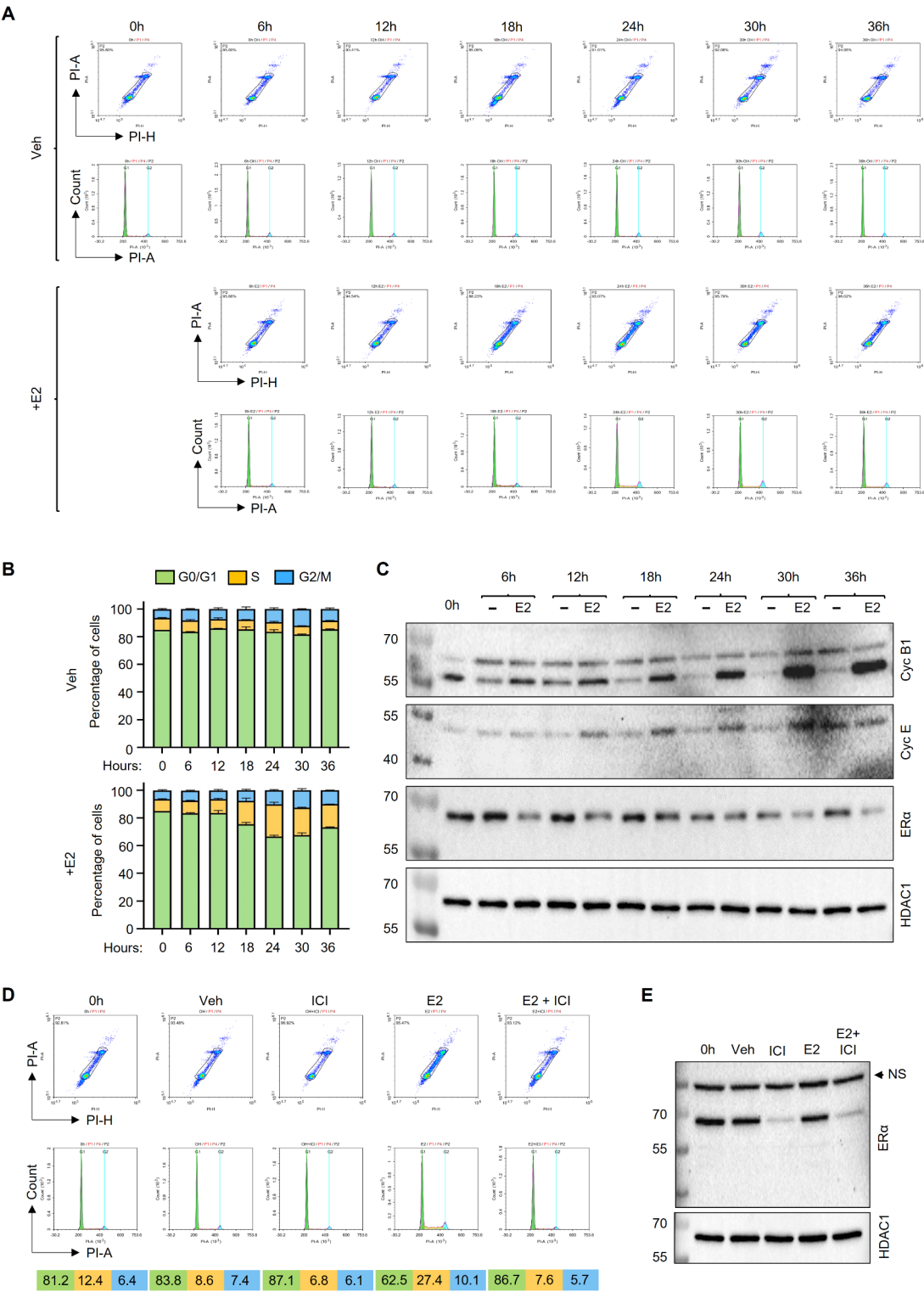


Fig. 6. Effects of 17β estradiol (E2) on cell cycle progression of T47D cells synchronized at G0/G1 by hormone withdrawal. (A–E) T47D cells were plated and grown in RPMI 1640 medium supplemented with 10% CD-FBS for 72 h with the medium change at 48 h. (A–C) Cells were subsequently maintained in the same medium containing 0.01% ethanol (EtOH) as vehicle control or 10^{-9} M E2 for 6 h intervals up to 36 h. Cells were collected with trypsinization. (A) A fraction of collected cells was subjected to the flow cytometry analysis (B) the results of which are represented with a bar graph of two independent replicates, and (C) the remaining cells were processed for WB analysis using an antibody for Cyclin B1 (Cyc B1), Cyclin E (Cyc E), ER α , or HDAC1. A representative image is shown. Molecular masses in kDa are indicated. (D & E) T47D cells synchronized at G0/G1 by hormone withdrawal (0 h) treated without (0.01% EtOH) or with 10^{-9} M E2 and/or 10^{-7} M ICI for 24 h. (D) Cells were collected with trypsinization and subjected to flow cytometry or (E) WB using an antibody for ER α or HDAC1. In A & C and D & E, representative images from the same experiment are shown. G0/G1, S, and G2/M indicate cell cycle phases. Molecular masses in kDa are indicated. NS designates an unspecific protein species detected with the ER α antibody.

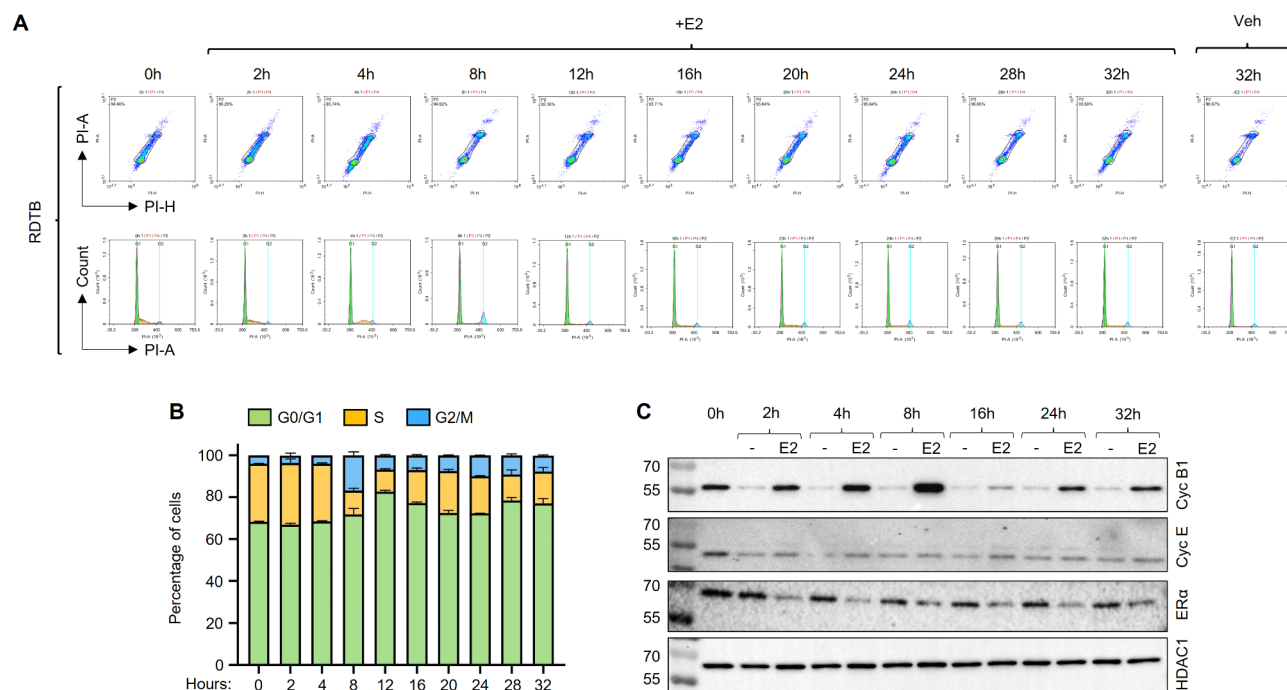


Fig. 7. Effects of 17β estradiol (E2) on cell cycle progression of T47D cells synchronized at the G1/S transition by CD-FBS and double thymidine block. (A & C) T47D cells grown in RPMI 1640 medium supplemented with 10% FBS for 72 h were incubated in RPMI 1640 medium containing 10% CD-FBS together with 2 mM thymidine for 14 h followed by washing the cells and re-incubating them in the same medium without thymidine for 12 h. Cells were re-incubated with fresh RPMI 1640 medium containing 10% CD-FBS and 2 mM thymidine for an additional 22 h. Cells were released from the double thymidine block (RDTB) by washing the cells and incubating with the same medium in the absence (0.01% EtOH) or presence of 10^{-9} M E2 for 2–4 h intervals up to 32 h. Cells at each time point were collected with trypsinization and (A) subjected to flow cytometry (B) with a bar graph representing the results of two independent experiments, and (C) to WB using antibodies for Cyclin B1 (Cyc B1), Cyclin E (Cyc E), ER α , or HDAC1. In A & C, representative images from the same experiment are shown. G0/G1, S, and G2/M indicate cell cycle phases. Molecular masses in kDa are indicated.

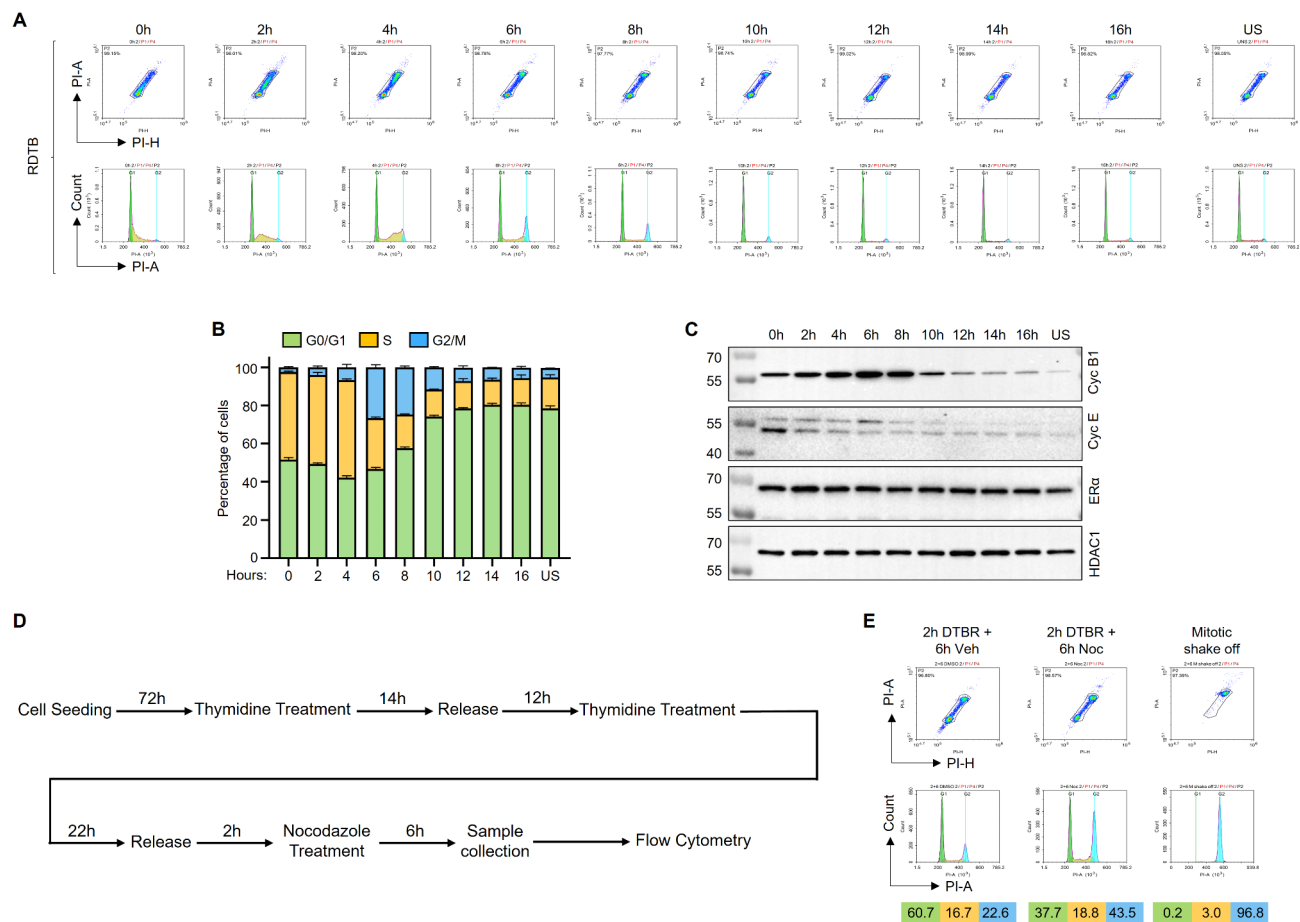


Fig. 8. Effects of the release of T47D cells from double thymidine block on cycle progression and phase enrichment. (A–C) T47D cells were grown in RPMI 1640 medium supplemented with 10% FBS for 72 h. Cells were incubated with RPMI 1640 medium supplemented with 10% FBS and with 2 mM thymidine for 14 h. Cells were released from the thymidine block in the same medium without thymidine for 12 h. Cells were re-incubated with fresh RPMI 1640 medium containing 10% FBS and 2 mM thymidine for an additional 22 h. Cells were subsequently released from the double thymidine block (RDTB) and incubated in the same growth medium without thymidine for 2 h intervals up to 16 h. Cells at each time point were collected with trypsinization and (A) subjected to flow cytometry analysis (B) with a bar graph representing the results of two independent experiments, and (C) to WB using an antibody for Cyclin B1 (Cyc B1), Cyclin E (Cyc E), ERα, or HDAC1. In A & C, representative images from the same experiment are shown. G0/G1, S, and G2/M indicate cell cycle phases. Molecular masses in kDa are indicated. US denotes unsynchronized cells. (D & E) T47D cells at 2 h release from the double thymidine block (RDTB) were incubated in fresh RPMI 1640 medium containing 10% FBS without (Veh) or with 0.3 μM nocodazole (Noc) for an additional 6 h. Cells were then collected by trypsinization or by mitotic shake-off for flow cytometry. G0/G1, S, and G2/M indicate cell cycle phases.

Data availability

All data generated or analysed during this study are included in this published article and its supplementary information files.

Received: 31 May 2024; Accepted: 13 February 2025

Published online: 18 February 2025

References

- Gookin, S. et al. A map of protein dynamics during cell-cycle progression and cell-cycle exit. *PLoS Biol.* **15**, (2017).
- Doenecke, D. Chromatin Dynamics during the cell cycle. *Chromatin Regul. Dynamics.* <https://doi.org/10.1016/B978-0-12-80339-5-1.00005-8> (2017).
- Liu, Y. et al. Transcriptional landscape of the human cell cycle. *Proc. Natl. Acad. Sci. U S A* **114**, (2017).
- Kheir, T. B. & Lund, A. H. Epigenetic dynamics across the cell cycle. *Essays Biochem.* **48**, (2010).
- Ayaz, G. et al. Dynamic transcriptional events mediated by estrogen receptor alpha. *Front. Bioscience - Landmark* **24**, (2019).
- Yaşar, P., Ayaz, G., User, S. D., Güpür, G. & Muyan, M. Molecular mechanism of estrogen–estrogen receptor signaling. *Reproductive Medicine and Biology* vol. 16 Preprint at (2017). <https://doi.org/10.1002/rmb2.12006>

7. Powell, C. E., Soto, A. M. & Sonnenschein, C. Identification and characterization of membrane estrogen receptor from MCF7 estrogen-target cells. *J. Steroid Biochem. Mol. Biol.* **77**, (2001).
8. Kampa, M. et al. Opposing effects of estradiol- and testosterone-membrane binding sites on T47D breast cancer cell apoptosis. *Exp. Cell. Res.* **307**, (2005).
9. Pedram, A., Razandi, M., Wallace, D. C. & Levin, E. R. Functional estrogen receptors in the mitochondria of breast cancer cells. *Mol. Biol. Cell.* **17**, (2006).
10. Karakas, B. et al. Mitochondrial estrogen receptors alter mitochondrial priming and response to endocrine therapy in breast cancer cells. *Cell. Death Discov.* **7**, (2021).
11. Prossnitz, E. R. & Barton, M. Estrogen biology: New insights into GPER function and clinical opportunities. *Molecular and Cellular Endocrinology* vol. 389 Preprint at (2014). <https://doi.org/10.1016/j.mce.2014.02.002>
12. Kumar, P. et al. Direct interactions with Gαi and Gβγ mediate nongenomic signaling by estrogen receptor α. *Mol. Endocrinol.* **21**, (2007).
13. Razandi, M., Pedram, A., Park, S. T. & Levin, E. R. Proximal events in signaling by plasma membrane estrogen receptors. *J. Biol. Chem.* **278**, (2003).
14. Sanchez, A. M. et al. Estrogen receptor-α promotes breast cancer cell motility and invasion via focal adhesion kinase and N-WASP. *Mol. Endocrinol.* **24**, (2010).
15. Harrington, W. R. et al. Estrogen dendrimer conjugates that preferentially activate extranuclear, nongenomic versus genomic pathways of estrogen action. *Mol. Endocrinol.* **20**, (2006).
16. Bourdeau, V. et al. Mechanisms of primary and secondary estrogen target gene regulation in breast cancer cells. *Nucleic Acids Res.* **36**, (2008).
17. Hah, N. et al. A rapid, extensive, and transient transcriptional response to estrogen signaling in breast cancer cells. *Cell* **145**, (2011).
18. Jagannathan, V. & Robinson-Rechavi, M. Meta-analysis of estrogen response in MCF-7 distinguishes early target genes involved in signaling and cell proliferation from later target genes involved in cell cycle and DNA repair. *BMC Syst. Biol.* **5**, (2011).
19. Davis, P. K., Ho, A. & Dowdy, S. F. Biological methods for cell-cycle synchronization of mammalian cells. *BioTechniques* vol. 30 Preprint at (2001). <https://doi.org/10.2144/01306rv01>
20. Ligasová, A. & Koberna, K. Strengths and weaknesses of cell synchronization protocols based on inhibition of DNA synthesis. *International Journal of Molecular Sciences* vol. 22 Preprint at (2021). <https://doi.org/10.3390/ijms221910759>
21. Eastman, A. E. & Guo, S. The palette of techniques for cell cycle analysis. *FEBS Letters* vol. 594 Preprint at (2020). <https://doi.org/10.1002/1873-3468.13842>
22. Yaşar, P., Ayaz, G. & Muyan, M. Estradiol-estrogen receptor α mediates the expression of the CXXC5 gene through the estrogen response element-dependent signaling pathway. *Sci. Rep.* **6**, (2016).
23. Ayaz, G. et al. CXXC5 as an unmethylated CpG dinucleotide binding protein contributes to estrogen-mediated cellular proliferation. *Sci. Rep.* **10**, (2020).
24. Lacroix, M. & Leclercq, G. Relevance of breast cancer cell lines as models for breast tumours: An update. *Breast Cancer Research and Treatment* vol. 83 Preprint at (2004). <https://doi.org/10.1023/B:BREA.0000014042.54925.c>
25. Dai, X., Cheng, H., Bai, Z. & Li, J. Breast cancer cell line classification and its relevance with breast tumor subtyping. *Journal of Cancer* vol. 8 Preprint at (2017). <https://doi.org/10.7150/jca.18457>
26. Aka, J. A. & Lin, S. X. Comparison of functional proteomic analyses of human breast cancer cell lines T47D and MCF7. *PLoS One* **7**, (2012).
27. Radde, B. N. et al. Bioenergetic differences between MCF-7 and T47D breast cancer cells and their regulation by oestradiol and tamoxifen. *Biochem. J.* **465**, (2015).
28. Smith, S. E. et al. Molecular characterization of breast cancer cell lines through multiple omic approaches. *Breast Cancer Res.* **19**, (2017).
29. Prall, O. W. J., Rogan, E. M. & Sutherland, R. L. Estrogen regulation of cell cycle progression in breast cancer cells. in *J. Steroid Biochem. Mol. Biol.* **65** (1998).
30. Katzenellenbogen, B. S., Kendra, K. L., Norman, M. J. & Berthois, Y. Proliferation, hormonal responsiveness, and estrogen receptor content of mcf-7 human breast cancer cells grown in the short-term and long-term absence of estrogens. *Cancer Res.* **47**, (1987).
31. Osborne, C. K., Boldt, D. H. & Estrada, P. Human breast cancer cell cycle synchronization by estrogens and antiestrogens in culture. *Cancer Res.* **44**, (1984).
32. Jakesz, R. et al. Influence of cell proliferation and cell cycle phase on expression of estrogen receptor in MCF-7 breast cancer cells. *Cancer Res.* **44**, (1984).
33. Doisneau-Sixou, S. F. et al. Estrogen and antiestrogen regulation of cell cycle progression in breast cancer cells. in *Endocr. Relat. Cancer* **10** (2003).
34. Musgrove, E. A. et al. Growth factor, steroid, and steroid antagonist regulation of cyclin gene expression associated with changes in T-47D human breast cancer cell cycle progression. *Mol. Cell. Biol.* **13**, (1993).
35. Sikora, M. J., Johnson, M. D., Lee, A. V. & Oesterreich, S. Endocrine response phenotypes are altered by charcoal-stripped serum variability. *Endocrinology* **157**, (2016).
36. Sutherland, R. L., Green, M. D., Hall, R. E., Reddel, R. R. & Taylor, I. W. Tamoxifen induces accumulation of MCF 7 human mammary carcinoma cells in the G0/G1 phase of the cell cycle. *Eur. J. Cancer Clin. Oncol.* **19**, (1983).
37. Dalvai, M. & Bystricky, K. Cell cycle and anti-estrogen effects synergize to regulate cell proliferation and ER target gene expression. *PLoS One* **5**, (2010).
38. Reichstein, I. S. et al. Replacing animal-derived components in in vitro test guidelines OECD 455 and 487. *Sci. Total Environ.* **868**, (2023).
39. Galavazi, G., Schenk, H. & Bootsma, D. Synchronization of mammalian cells in vitro by inhibition of the DNA synthesis. I. optimal conditions. *Exp. Cell. Res.* **41**, (1966).
40. Galavazi, G. & Bootsma, D. Synchronization of mammalian cells in vitro by inhibition of the DNA synthesis. II. Population dynamics. *Exp. Cell. Res.* **41**, (1966).
41. Galgano, P. J. & Schildkraut, C. L. G1/S phase synchronization using double thymidine synchronization. *Cold Spring Harb Protoc* (2006). (2006).
42. Chen, G. & Deng, X. Cell synchronization by double thymidine block. *Bio Protoc.* **8**, (2018).
43. Muyan, M. et al. Fusion estrogen receptor proteins: toward the development of receptor-based agonists and antagonists. *Mol. Cell. Endocrinol.* **182**, (2001).
44. Rajendran, K. G., Lopez, T. & Parikh, I. Estrogenic effect of phenol red in MCF-7 cells is achieved through activation of estrogen receptor by interacting with a site distinct from the steroid binding site. *Biochem. Biophys. Res. Commun.* **142**, (1987).
45. Berthois, Y., Katzenellenbogen, J. A. & Katzenellenbogen, B. S. Phenol red in tissue culture media is a weak estrogen: implications concerning the study of estrogen-responsive cells in culture. *Proc. Natl. Acad. Sci. U S A* **83**, (1986).
46. Bindal, R. D., Carlson, K. E., Katzenellenbogen, B. S. & Katzenellenbogen, J. A. Lipophilic impurities, not phenolsulfonphthalein, account for the estrogenic activity in commercial preparations of phenol red. *J. Steroid Biochem.* **31**, (1988).
47. Bindal, R. D. & Katzenellenbogen, J. A. Bis(4-hydroxyphenyl)[2-(phenoxy-sulfonyl)phenyl]methane: isolation and structure elucidation of a novel estrogen from commercial preparations of phenol red (phenolsulfonphthalein). *J. Med. Chem.* **31**, (1988).

48. Welshons, W. V., Wolf, M. F., Murphy, C. S. & Jordan, V. C. Estrogenic activity of phenol red. *Mol. Cell. Endocrinol.* **57**, 169–178 (1988).
49. Zugmaier, G. et al. Tissue culture conditions determine the effects of estrogen and growth factors on the anchorage independent growth of human breast cancer cell lines. *J. Steroid Biochem. Mol. Biol.* **39**, (1991).
50. Moreno-Cuevas, J. E. & Sirbasku, D. A. Estrogen mitogenic action. III. Is phenol red a 'red herring'? *Vitro Cell. Dev. Biol. Anim.* **36**, (2000).
51. Frederiksen, H. et al. Sex-specific estrogen levels and reference intervals from infancy to late adulthood determined by LC-MS/MS. *J. Clin. Endocrinol. Metab.* **105**, (2020).
52. Huang, J. et al. Binding of estrogen receptor β to estrogen response element in situ is independent of estradiol and impaired by its amino terminus. *Mol. Endocrinol.* **19**, (2005).
53. Berry, M., Nunez, A. M. & Chambon, P. Estrogen-responsive element of the human pS2 gene is an imperfectly palindromic sequence. *Proc. Natl. Acad. Sci. U S A* **86**, (1989).
54. Jordan, V. C. Tamoxifen as the first targeted long-term adjuvant therapy for breast cancer. *Endocrine-Related Cancer* vol. 21 Preprint at (2014). <https://doi.org/10.1530/ERC-14-0092>
55. Jordan, V. C. & Morrow, M. Tamoxifen, raloxifene, and the prevention of breast cancer. *Endocrine Reviews* vol. 20 Preprint at (1999). <https://doi.org/10.1210/er.20.3.253>
56. Robertson, J. F. R. & Faslodex (ICI 182,780), a novel estrogen receptor downregulator - future possibilities in breast cancer. in *J. Steroid Biochem. Mol. Biol.* **79** (2001).
57. Robertson, J. F. R. ICI 182,780 (Fulvestrant™) - the first oestrogen receptor down-regulator - current clinical data. *Br. J. Cancer* **85**, (2001).
58. Gstraunthaler, G., Lindl, T. & Van Der Valk, J. A plea to reduce or replace fetal bovine serum in cell culture media. *Cytotechnology* vol. 65 Preprint at (2013). <https://doi.org/10.1007/s10616-013-9633-8>
59. van der Valk, J. Fetal bovine serum—a cell culture dilemma. *Science* vol. 375 Preprint at (2022). <https://doi.org/10.1126/science.abm1317>
60. Lee, D. Y. et al. Review of the current research on fetal bovine serum and the development of cultured meat. *Food Science of Animal Resources* vol. 42 Preprint at (2022). <https://doi.org/10.5851/kosfa.2022.e46>
61. Cao, Z. et al. Effects of resin or charcoal treatment on fetal bovine serum and bovine calf serum. *Endocr. Res.* **34**, (2009).
62. Soto, A. M. & Sonnenschein, C. The role of estrogens on the proliferation of human breast tumor cells (MCF-7). *J. Steroid Biochem.* **23**, (1985).
63. Yu, H. & Yao, X. Cyclin B1: conductor of mitotic symphony orchestra. *Cell. Res.* **18**, (2008).
64. Hwang, H. C. & Clurman, B. E. Cyclin E in normal and neoplastic cell cycles. *Oncogene* vol. 24 Preprint at (2005). <https://doi.org/10.1038/sj.onc.1208613>
65. Wijayarathne, A. L. & McDonnell, D. P. The human estrogen receptor- α is a ubiquitinated protein whose stability is affected differentially by agonists, antagonists, and selective estrogen receptor modulators. *J. Biol. Chem.* **276**, (2001).
66. Alarid, E. T., Bakopoulos, N. & Solodin, N. Proteasome-mediated proteolysis of estrogen receptor: a novel component in autologous down-regulation. *Mol. Endocrinol.* **13**, (1999).
67. Fan, M., Bigsby, R. M. & Nephew, K. P. The NEDD8 pathway is required for proteasome-mediated degradation of human estrogen receptor (ER)- α and essential for the antiproliferative activity of ICI 182,780 in ER α -positive breast cancer cells. *Mol. Endocrinol.* **17**, (2003).
68. McDonnell, D. P. & Wardell, S. E. The molecular mechanisms underlying the pharmacological actions of ER modulators: Implications for new drug discovery in breast cancer. *Current Opinion in Pharmacology* vol. 10 Preprint at (2010). <https://doi.org/10.1016/j.coph.2010.09.007>
69. Jordan, V. C. & O'Malley, B. W. Selective estrogen-receptor modulators and antihormonal resistance in breast cancer. *Journal of Clinical Oncology* vol. 25 Preprint at (2007). <https://doi.org/10.1200/JCO.2007.11.3886>
70. Brzozowski, A. M. et al. Molecular basis of agonism and antagonism in the oestrogen receptor. *Nature* **389**, (1997).
71. Shiau, A. K. et al. The structural basis of estrogen receptor/coactivator recognition and the antagonism of this interaction by tamoxifen. *Cell* **95**, (1998).
72. Keyomarsi, K., Sandoval, L., Band, V. & Pardee, A. B. Synchronization of tumor and normal cells from G1 to multiple cell cycles by lovastatin. *Cancer Res.* **51**, (1991).
73. Hengst, L., Dulic, V., Slingerland, J. M., Lees, E. & Reed, S. I. A cell cycle-regulated inhibitor of cyclin-dependent kinases. *Proc. Natl. Acad. Sci. U S A* **91**, (1994).
74. Rao, S. et al. Lovastatin-mediated G1 arrest is through inhibition of the proteasome, independent of hydroxymethyl glutaryl-CoA reductase. *Proc. Natl. Acad. Sci. U S A* **96**, (1999).
75. Moghadam-Kamrani, S. J. & Keyomarsi, K. Synchronization of the cell cycle using lovastatin. *Cell. Cycle* **7**, (2008).
76. Dijkwel, P. A. & Hamlin, J. L. Initiation of DNA replication in the dihydrofolate reductase locus is confined to the early S period in CHO cells synchronized with the plant amino acid mimosine. *Mol. Cell. Biol.* **12**, (1992).
77. Krude, T. Mimosine arrests proliferating human cells before onset of DNA replication in a dose-dependent manner. *Exp. Cell. Res.* **247**, (1999).
78. Lee, J. & Gollahon, L. Mitotic perturbations induced by Nek2 overexpression require interaction with TRF1 in breast cancer cells. *Cell. Cycle* **12**, (2013).
79. Wakeling, A. E., Newbould, E. & Peters, S. W. Effects of antioestrogens on the proliferation of MCF-7 human breast cancer cells. *J. Mol. Endocrinol.* **2**, (1989).
80. Butler, W. B. & Kelsey, W. H. Effects of tamoxifen and 4-hydroxytamoxifen on synchronized cultures of the human breast cancer cell line MCF-7. *Breast Cancer Res. Treat.* **11**, (1988).
81. Lykkesfeldt, A. E., Larsen, J. K., Christensen, I. J. & Briand, P. Effects of the antioestrogen tamoxifen on the cell cycle kinetics of the human breast cancer cell line, MCF-7. *Br. J. Cancer* **49**, (1984).
82. Carroll, J. S., Prall, O. W. J., Musgrove, E. A. & Sutherland, R. L. A pure estrogen antagonist inhibits cyclin E-Cdk2 activity in MCF-7 breast cancer cells and induces accumulation of p130-E2F4 complexes characteristic of quiescence. *J. Biol. Chem.* **275**, (2000).
83. Scholzen, T. & Gerdes, J. The Ki-67 protein: From the known and the unknown. *Journal of Cellular Physiology* vol. 182 Preprint at (2000). [https://doi.org/10.1002/\(SICI\)1097-4652\(200003\)182:3<311::AID-JCP1>3.0.CO;2-9](https://doi.org/10.1002/(SICI)1097-4652(200003)182:3<311::AID-JCP1>3.0.CO;2-9)
84. Beresford, M. J., Wilson, G. D. & Makris, A. Measuring proliferation in breast cancer: Practicalities and applications. *Breast Cancer Research* vol. 8 Preprint at (2006). <https://doi.org/10.1186/bcr1618>
85. Ikegami, S. et al. Aphidicolin prevents mitotic cell division by interfering with the activity of DNA polymerase- α [18]. *Nature* vol. 275 Preprint at (1978). <https://doi.org/10.1038/275458a0>
86. Zhu, H. et al. Induction of S-phase arrest and p21 overexpression by a small molecule 2[[3-(2,3-dichlorophenoxy)propyl]amino] ethanol in correlation with activation of ERK. *Oncogene* **23**, (2004).
87. Bai, B. et al. Small molecule 2,3DCPE induces S phase arrest by activating the ATM/ATRChk1Cdc25A signaling pathway in DLD-1 colon cancer cells. *Oncol. Lett.* **20**, (2020).
88. Cheung, H. T. & Terry, D. S. Effects of nocodazole, a new synthetic microtubule inhibitor, on movement and spreading of mouse peritoneal macrophages. *Cell. Biol. Int. Rep.* **4**, (1980).
89. Schorl, C. & Sedivy, J. M. Analysis of cell cycle phases and progression in cultured mammalian cells. *Methods* **41**, (2007).

90. Fuentes-Antrás, J., Bedard, P. L. & Cescon, D. W. Seize the engine: emerging cell cycle targets in breast cancer. *Clin. Transl. Med.* **14**, (2024).
91. Schafer, K. A. The cell cycle: A review. *Veterinary Pathology* vol. 35 Preprint at (1998). <https://doi.org/10.1177/030098589803500601>
92. Piezzo, M. et al. Targeting cell cycle in breast cancer: CDK4/6 inhibitors. *International Journal of Molecular Sciences* vol. 21 Preprint at (2020). <https://doi.org/10.3390/ijms21186479>
93. Perrone, M. et al. Advances in pharmacotherapies that target the cell cycle for treatment of breast cancer: where are we at today? *Expert Opinion on Pharmacotherapy* vol. 24 Preprint at (2023). <https://doi.org/10.1080/14656566.2023.2201373>
94. Lord, C. J. & Ashworth, A. PARP inhibitors: Synthetic lethality in the clinic. *Science* vol. 355 Preprint at (2017). <https://doi.org/10.1126/science.aam7344>
95. Paluch-Shimon, S. & Evron, E. Targeting DNA repair in breast cancer. *Breast* **47**, (2019).
96. Correia, A. S., Gärtner, F. & Vale, N. Drug combination and repurposing for cancer therapy: the example of breast cancer. *Heliyon* vol. 7 Preprint at (2021). <https://doi.org/10.1016/j.heliyon.2021.e05948>
97. Aggarwal, S., Verma, S. S., Aggarwal, S. & Gupta, S. C. Drug repurposing for breast cancer therapy: Old weapon for new battle. *Seminars in Cancer Biology* vol. 68 Preprint at (2021). <https://doi.org/10.1016/j.semcancer.2019.09.012>
98. Khan, M. M., Yalamarty, S. S. K., Rajmalani, B. A. & Filipczak, N. & Torchilin, V. P. recent strategies to overcome breast cancer resistance. *Crit. Rev. Oncol. Hematol.* **197**, (2024).
99. Gu, G., Dustin, D. & Fuqua, S. A. Targeted therapy for breast cancer and molecular mechanisms of resistance to treatment. *Current Opinion in Pharmacology* vol. 31 Preprint at (2016). <https://doi.org/10.1016/j.coph.2016.11.005>
100. Rakha, E. A., Tse, G. M. & Quinn, C. M. An update on the pathological classification of breast cancer. *Histopathology* vol. 82 Preprint at (2023). <https://doi.org/10.1111/his.14786>
101. Neve, R. M. et al. A collection of breast cancer cell lines for the study of functionally distinct cancer subtypes. *Cancer Cell.* **10**, (2006).
102. Weigelt, B., Geyer, F. C. & Reis-Filho, J. S. Histological types of breast cancer: How special are they? *Molecular Oncology* vol. 4 Preprint at (2010). <https://doi.org/10.1016/j.molonc.2010.04.004>
103. Huang, J., Li, X., Hilf, R., Bambara, R. A. & Muyan, M. Molecular basis of therapeutic strategies for breast cancer. *Current Drug Targets: Immune, Endocrine and Metabolic Disorders* vol. 5 Preprint at (2005). <https://doi.org/10.2174/156800805774912944>
104. Osborne, C. K., Hobbs, K. & Trent, J. M. Biological differences among MCF-7 human breast cancer cell lines from different laboratories. *Breast Cancer Res. Treat.* **9**, (1987).
105. Burdall, S. E., Hanby, A. M., Lansdown, M. R. J. & Speirs, V. Breast cancer cell lines: Friend or foe? *Breast Cancer Research* vol. 5 Preprint at (2003). <https://doi.org/10.1186/bcr577>
106. Kao, J. et al. Molecular profiling of breast cancer cell lines defines relevant tumor models and provides a resource for cancer gene discovery. *PLoS One* **4**, (2009).

Acknowledgements

This study was supported by the Scientific and Technological Research Council of Türkiye (TUBITAK) under grant numbers 121Z346 and 114Z243. We thank TUBITAK for their support. We also express our gratitude to Dr. Aytekin Akyol for sharing reagents with us.

Author contributions

PT, HA, ÖDD, and BB have contributed equally. PT, HA, ÖDD, and BB have contributed to data curation, formal analysis, investigation, methodology, and writing original drafts and editing. GT, ÇEO, and PY have contributed to the investigation and methodology. HBA and MM have contributed to formal analysis, supervision, funding acquisition, methodology, writing original drafts and editing, and project administration. All authors have reviewed and approved the final manuscript.

Declarations

Competing interests

The authors declare no competing interests.

Additional information

Supplementary Information The online version contains supplementary material available at <https://doi.org/10.1038/s41598-025-90456-8>.

Correspondence and requests for materials should be addressed to M.M.

Reprints and permissions information is available at www.nature.com/reprints.

Publisher's note Springer Nature remains neutral with regard to jurisdictional claims in published maps and institutional affiliations.

Open Access This article is licensed under a Creative Commons Attribution-NonCommercial-NoDerivatives 4.0 International License, which permits any non-commercial use, sharing, distribution and reproduction in any medium or format, as long as you give appropriate credit to the original author(s) and the source, provide a link to the Creative Commons licence, and indicate if you modified the licensed material. You do not have permission under this licence to share adapted material derived from this article or parts of it. The images or other third party material in this article are included in the article's Creative Commons licence, unless indicated otherwise in a credit line to the material. If material is not included in the article's Creative Commons licence and your intended use is not permitted by statutory regulation or exceeds the permitted use, you will need to obtain permission directly from the copyright holder. To view a copy of this licence, visit <http://creativecommons.org/licenses/by-nc-nd/4.0/>.

© The Author(s) 2025